



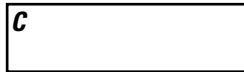
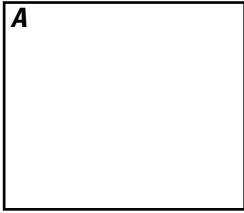
Earthquake Hazards Program

Induced Seismicity Strategic Vision

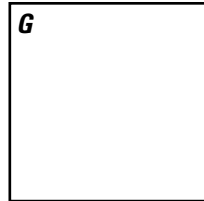
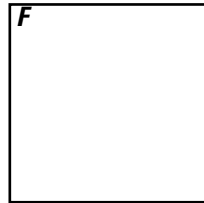


Circular 1509

U.S. Department of the Interior
U.S. Geological Survey



Front Cover. *A*, House damage in central Oklahoma from the magnitude *M*5.7 earthquake on November 6, 2011. U.S. Geological Survey photograph by Brian Sherrod. *B*, Cooling towers in operation during the energy production and fluid reinjection process at a flash steam geothermal power plant in California. U.S. Geological Survey photograph by Andrew Barbour. *C*, Two water tanker trucks at a wastewater disposal site in Colorado. U.S. Geological Survey photograph by Justin Rubinstein. *D*, Global positioning system (GPS) station P507 in the Network of the Americas, which has been measuring ground displacements since 2005 at the southern end of the Salton Sea in California, using the Global Navigation Satellite System (GNSS). U.S. Geological Survey photograph by Andrew Barbour.



Back Cover. *E*, A U.S. Geological Survey-operated nodal seismic station (orange flag in the foreground) installed in Grant County, Oklahoma, in 2016, as part of an array of more than 1,800 seismic stations used to study earthquakes induced by wastewater injection. U.S. Geological Survey photograph by Elizabeth Cochran. *F*, Oil covered well-head at a wastewater disposal site in Oklahoma. U.S. Geological Survey photograph by Justin Rubinstein. *G*, U.S. Geological Survey operated pore-pressure observatory in Oklahoma that measures fluid-pressure changes in a deep injection reservoir. Seismometers are co-located at the observatory's surface. U.S. Geological Survey photograph by Andrew Barbour.

Earthquake Hazard Program

Induced Seismicity Strategic Vision

By Elizabeth S. Cochran, Justin L. Rubinstein, Andrew J. Barbour, and J. Ole Kaven

Circular 1509

U.S. Department of the Interior
U.S. Geological Survey

U.S. Geological Survey, Reston, Virginia: 2024

For more information on the USGS—the Federal source for science about the Earth, its natural and living resources, natural hazards, and the environment—visit <https://www.usgs.gov> or call 1–888–392–8545. For an overview of USGS information products, including maps, imagery, and publications, visit <https://store.usgs.gov/> or contact the store at 1–888–275–8747.

Any use of trade, firm, or product names is for descriptive purposes only and does not imply endorsement by the U.S. Government.

Although this information product, for the most part, is in the public domain, it also may contain copyrighted materials as noted in the text. Permission to reproduce [copyrighted items](#) must be secured from the copyright owner.

Suggested citation:

Cochran, E.S., Rubinstein, J.L., Barbour, A.J., and Kaven, J.O., 2024, Induced seismicity strategic vision: U.S. Geological Survey Circular 1509, 39 p., <https://doi.org/10.3133/cir1509>.

Acknowledgments

Work presented in this circular was funded in part by the Department of Energy and the California Energy Commission.

This circular benefitted from input from many members of the U.S. Geological Survey's induced seismicity community, including Rufus Catchings, Jemile Erdem, Mark Goldman, Stephen Hickman, Andrea Llenos, David Lockner, Jens-Erik Lundstern, Tamara Jeppson, Kathryn Materna, Art McGarr, Walter Mooney, Evelyn Roeloffs, Robert Skoumal, William Yeck, and Clara Yoon.

Additional thanks go to Nick Beeler, Harley Benz, Jessica Murray, and members of the Earthquake Hazards Program Council for constructive feedback that improved this report.

Gavin Hayes and the permanent and acting center directors from the Earthquake and Geological Hazards Science Centers (2020-24) were instrumental in shepherding the circular through its development and review steps.

Contents

Acknowledgments	III	Downhole Pressure Monitoring	18
Executive Summary	1	Numerical Modeling.....	20
Introduction.....	2	Assessment of Seismic Hazard	20
State of Knowledge	4	Maximum Magnitude Expectations	20
Oil and Gas	4	Ground Motions.....	21
Geothermal.....	7	Short-Term Earthquake Hazard Forecast Models.....	21
Geologic CO ₂ Sequestration	9	Emerging Focus Areas	24
Broader Partnerships and Communication	11	Permian Basin	24
Prioritized Areas for Advancements	11	Frontier Observatory for Research in Geothermal Energy	26
Seismic Monitoring and Analysis	12	Limitations and Opportunities for Innovation	26
Earthquake Monitoring	12	Limitations	26
Enhanced Earthquake Catalogs	13	Industrial Data	27
Sequence Behavior	13	Geological Data.....	27
Source Properties.....	15	Seismological Data.....	27
Geodetic Monitoring and Analysis	15	Opportunities for Innovation	28
Geophysical Studies of Geologic Structure and Physical Properties ..	16	Oil and Gas	28
Fault Identification from Seismicity	16	Geothermal.....	29
Stress State.....	16	Geologic CO ₂ Sequestration.....	30
Laboratory Rock Mechanics Experiments and Analysis	18	Summary.....	31
Geomechanical and Hydrological Monitoring and Models.....	18	References Cited.....	32

Figures

- | | |
|--|----|
| 1. Schematic showing how earthquakes can be induced by stress changes along faults owing to injection or removal of fluids from the subsurface | 3 |
| 2. Simplified diagrams of oil-field operations..... | 5 |
| 3. Rate of magnitude (M) ≥ 3 earthquakes in the central United States from 2000 to 2022 | 6 |
| 4. Map showing locations of geothermal wells and major faults in California | 8 |
| 5. Map showing locations of current and pending permits for geologic CO ₂ sequestration wells | 10 |
| 6. Map showing distribution of foreshocks, mainshocks, and aftershocks from clustering analysis in Grant County, Oklahoma | 14 |
| 7. Map showing fault structures of the 2011 Prague, Oklahoma, earthquake sequence identified with FaultID using aftershock locations..... | 17 |
| 8. Map and timeseries graphs showing the shear strain response of the Arbuckle Group reservoir in Oklahoma to the 2018 moment magnitude 7.9 Kodiak, Alaska, earthquake, ~40° away..... | 19 |
| 9. Comparison of peak ground accelerations forecast in central Oklahoma and southern Kansas | 22 |
| 10. Bar graph showing seismicity rate increases in the region of the Permian Basin, including the Delaware Basin..... | 25 |

Abbreviations

ANSS	Advanced National Seismic System	ISP	Induced Seismicity Project
AQMS	ANSS Quake Monitoring System	ISRO	Indian Space Research Organization
DOE	Department of Energy	M	magnitude
EGS	engineered geothermal systems	M_w	moment magnitude
EHP	Earthquake Hazards Program	M_{\max}	maximum magnitude
EPA	Environmental Protection Agency	NASA	National Aeronautics and Space Administration
ETAS	epidemic-type aftershock sequence	NEIC	National Earthquake Information Center
FEM	finite element model	NISAR	NASA-ISRO SAR
FORGE	Frontier Observatory for Research in Geothermal Energy	NWIS	National Water Information System
GCS	geologic CO ₂ sequestration	SAGE	Seismological Facility for the Advancement of Geoscience
GMM	ground-motion model	SAR	synthetic aperture radar
GNSS	global navigation satellite system	THMC	thermal-hydrological-mechanical-chemical
IBDP	Illinois Basin Decatur Project	UAV	Uninhabited Aerial Vehicle
ICCS	Illinois Industrial Carbon Capture and Storage Project	USGS	U.S. Geological Survey
InSAR	interferometric synthetic aperture radar		



Induced Seismicity Strategic Vision

By Elizabeth S. Cochran, Justin L. Rubinstein, Andrew J. Barbour, and J. Ole Kaven

Executive Summary

The U.S. Geological Survey has a long history of contributions to the understanding and resolution of various scientific questions related to earthquakes associated with human activities, referred to as induced seismicity. Work started with the Rocky Mountain Arsenal studies in the 1960's (Healy and others, 1968) when it was first discovered that fluid waste-disposal operations can cause earthquakes. U.S. Geological Survey work on induced seismicity continued in the intervening years but expanded dramatically in the early 2010s. Disposal of large volumes of wastewater, a byproduct of oil and gas production, into the subsurface caused an exponential increase in earthquakes in the central United States, including earthquakes that caused damage to buildings and infrastructure in nearby communities. Established in 2012 within the Earthquake Hazards Program (EHP), the Induced Seismicity Project (ISP) examines earthquakes that are induced by human activities to assess and mitigate the hazards associated with induced earthquakes as well as understand the conditions and processes controlling induced and natural earthquake generation and recurrence. The ISP examines instances of suspected induced earthquakes, in real-time and retrospectively, to assess the probabilistic hazard and investigate possibilities for reducing that hazard, something currently not possible with natural earthquake activity. The ISP has many synergies with work across multiple areas of EHP, including earthquake monitoring, hazard mitigation, and fundamental research into earthquake processes.

In this report, background on induced seismicity and an overview of the state of knowledge is provided in three topical task areas: (1) oil and gas, (2) geothermal, and (3) geologic CO₂ sequestration. This report then presents the EHP's goals, strategies, and approaches—primarily focused on work in the ISP—for understanding the conditions that lead to induced seismicity, mitigating the associated hazards, and assisting the Nation in meeting its future needs in energy production and mitigation of climate change. Finally, the key limitations and opportunities for innovation are outlined at the end of the report.

The overarching questions that guided the development of our research strategies and approaches are as follows:

- How can seismicity that is induced by industrial activities be better distinguished from natural processes, particularly in regions with higher rates of natural seismicity?
- Can faults that may be at increased hazard for induced seismicity be identified based on existing fault structures, past earthquake activity, local stress conditions, or other information?
- What geologic and operational conditions control the occurrence, spatial and temporal evolution, maximum magnitude, ground shaking, and other characteristics of induced seismic sequences?
- What roles do surface and subsurface deformation, aseismic slip, and other processes play in the occurrence of injection-induced earthquakes?
- How can induced seismicity be better forecasted to support the Nation's energy production and climate mitigation goals while limiting related earthquake hazards?

Introduction

Human activities that cause subsurface stress changes have long been linked to the occurrence of earthquakes. For instance, injecting or extracting fluids during the processes of recovering hydrocarbons, generating geothermal energy, or geologically sequestering CO₂ can, in some instances, cause earthquakes (National Research Council, 2013). Earthquakes that result from human activities are referred to as induced earthquakes throughout this report. Work is focused on induced earthquakes that are caused when fluids injected into or removed from the subsurface change the stresses along faults because those currently dominate the induced seismic hazard in the United States (Petersen and others, 2015). Stress changes may include direct fluid pressure changes within fault zones and indirect stress changes resulting from deformation of the rock around them (fig. 1). A component of the U.S. Geological Survey (USGS) Earthquake Hazards Program (EHP) is to examine the causes of induced seismicity and provide information to stakeholders that can be used to mitigate their effects.

Much of the effort in the EHP to understand and mitigate the hazard from induced seismicity is undertaken by the Induced Seismicity Project (ISP). Induced seismicity-related research applies to many areas of the EHP; as such, several synergies exist with other projects and efforts within the program. For example, the EHP comprises projects dedicated to research into the physics of earthquake initiation, rupture, and arrest of natural earthquakes; understanding sources and impacts of strong ground motions; forecasting of seismic hazard; and other topics. The ISP includes work in these areas, although the project primarily focuses on earthquakes induced by industrial activities.

The ISP is divided into 4 tasks that focus on induced seismicity: oil and gas, geothermal, CO₂ sequestration, and monitoring. The main ISP activities within these tasks are as follows: (1) seismic monitoring and analysis, (2) geodetic monitoring and analysis, (3) geophysical

studies of geologic structure and physical properties, (4) laboratory rock mechanics experiments and analysis, (5) geomechanical and hydrological monitoring and models, and (6) assessment of seismic hazard. These activities may reveal the nature of the earthquake sources that are induced by industrial activities. Hydrological and geomechanical field measurements and modeling are used to determine the stress and hydrologic conditions at depth, which, in comparison with geophysical site characterization studies and seismological observables, provide a clearer picture of the faulting conditions and processes controlling induced seismicity (Ge and Saar, 2022). In addition to focused case studies (McGarr and others, 2002), cataloging the presence or absence of earthquakes induced by injection activities yields critical information regarding conditions favorable for induced seismicity (Suckale, 2009; Keranen and others, 2014; Zang and others, 2014; Hincks and others, 2018; Skoumal and others, 2018; Ries and others, 2020).

Insights into the behavior of induced seismicity have been translated into recommendations for more effective estimates of hazard (Petersen and others, 2015; 2016; 2017; 2018) as well as management of deep-injection activities (Majer, 2013; Folger and Tiemann, 2016; White and others, 2016). ISP collects and merges earthquake information, geologic data, and industry-provided operational data to provide timely information about present and future earthquake hazards. To assess hazard, statistical and physics-based models are developed and tested to accurately forecast changes in seismicity rates caused by injection activities (Petersen and others, 2015; 2016; 2017; 2018; Norbeck and Rubinstein, 2018; Rubinstein and others, 2021). These may be used by operators and regulators to design hazard mitigation strategies. Maps of expected ground motion probabilities across regions of induced seismicity are based on models of how injection alters the local seismic hazard (Petersen and others, 2015; 2016; 2017; 2018). These same forecasts may be used

to assess the likelihood of significant consequences (for example, injury or structural damage) at critical facilities (for example, hospitals, fire stations, schools), lifelines (for example, water, power, and transportation infrastructure), or other sites of interest. When shown to have reasonable forecast capability, these forecasts of expected ground motion probabilities provide information that may be useful for emergency management officials and for defining operational procedures that, for example, could appropriately balance industry needs against seismic hazard. The ability to accurately estimate short-term seismic hazard presented by injection activities has dramatically improved throughout the past decade as a direct result of improved monitoring and research efforts by the USGS and through collaborations with external partners.

Studies of induced seismicity may also inform about the physics of earthquake failure through improved knowledge of the conditions controlling earthquake generation and recurrence. We examine the processes that control earthquake rates, locations, magnitude distribution, and other factors through integration of high-resolution earthquake locations and source parameters, subsurface physical properties, and fluid injection rates and pressures.

An objective of studying induced seismicity is to be able to forecast the distribution of earthquakes, including the maximum magnitude, that is likely to result from industrial operations, whether related to oil and gas, geothermal energy, or CO₂ sequestration. Understanding whether and how production or injection operations interact with nearby pre-existing faults to influence the occurrence of earthquakes by, for example, causing them to occur earlier than

they might have otherwise may improve forecast accuracy. Using knowledge of stresses, fluid pressure, rock properties, geologic and hydrologic structure, and temperature at depths where induced earthquakes occur, we can better understand the behavior of both naturally occurring and induced earthquakes.

The ISP has a robust seismic, geodetic, and pore pressure monitoring program. Rapid, short-term deployments are undertaken for situational awareness

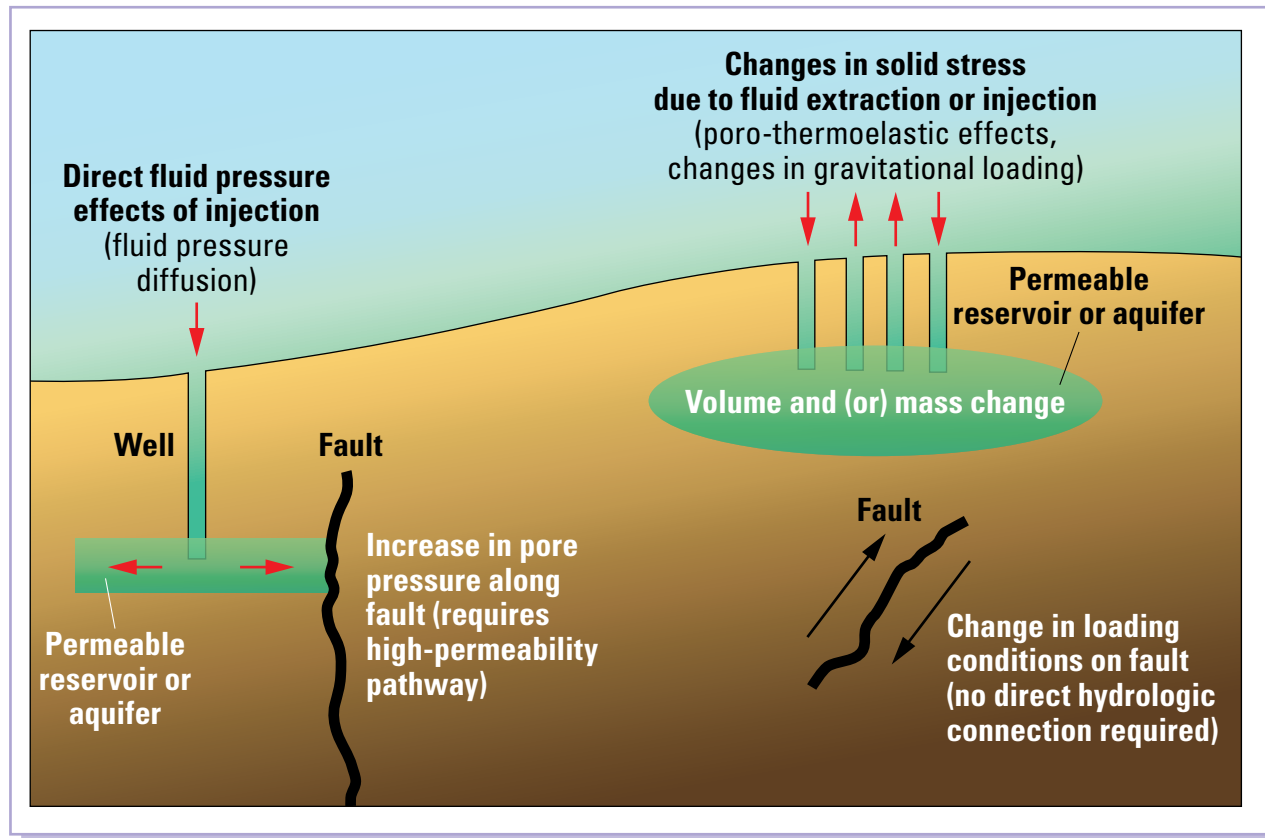


Figure 1. Schematic showing how earthquakes can be induced by stress changes along faults owing to injection or removal of fluids from the subsurface. Stress changes may include direct fluid pressure changes within fault zones and indirect stress changes resulting from deformation of the rock around them. Modified from Ellsworth (2013).

and to collect ephemeral data such as aftershock sequences. Dedicated, longer-term field deployments are also used with the goal of better understanding sustained seismic, geodetic, and pore pressure changes in areas of injection activities. The ability to deploy observational networks has contributed substantially to an improved understanding of the behavior and effects of fluid-induced seismicity. Deployments are often undertaken by the USGS and its state and academic partners.

State of Knowledge

Oil and Gas

The United States is experiencing a significant increase in oil and gas production owing to the development of technology that has enabled production from previously inaccessible or economically infeasible resources—referred to as unconventional reservoirs (Ellsworth, 2013). These operations yield considerable quantities of coproduced wastewater composed of formation brines and the fluids injected to enhance permeability and production efficiency (for example, Murray, 2015). Because wastewater is generally expensive to clean and reuse, it is commonly injected into deep formations for disposal instead, an activity that can induce earthquakes (Ellsworth, 2013; Rubinstein and Mahani, 2015). Although the probability of a given disposal well inducing earthquakes large enough to be felt is small, the combined effect of many wells adds significantly to the seismic hazard in a region, especially in the central United States, where natural seismicity rates are low (Petersen and others, 2015; 2016; 2017; 2018). Earthquakes large enough to cause damage can also be induced by hydraulic fracturing, conventional oil and gas production, water flooding, and carbon dioxide injection to enhance production in depleted fields (fig. 2) (Rubinstein and Mahani, 2015). A major challenge for the ISP is to understand how activities related to oil and gas production may induce earthquakes, and to account for their contributions to the total seismic hazard in a realistic way.

Changes in oil and gas operations have increased the rate of seismic events in parts of the United States. For more than three decades prior to 2008, about 25 magnitude $M \geq 3$ earthquakes occurred per year in the Central United States. Earthquake rates increased rapidly to more than 1,000 $M \geq 3$ earthquakes in 2015, following the expansion of oil and gas operations in the central United States (fig. 3) (U.S. Geological Survey, 2017). The vast majority of these recent earthquakes

have been associated with increased wastewater disposal into deep wells and, to a lesser degree, hydraulic fracturing stimulations (Ellsworth, 2013; Rubinstein and Mahani, 2015; Skoumal and Trugman, 2021). Hazard forecasts based on the increased seismicity rates have shown that hazard increased in areas of induced seismicity in the central United States approximately tenfold compared to background hazard (Petersen and others, 2016). Earthquake rates decreased to less than 300 $M \geq 3$ earthquakes per year in the period from 2018 to 2022 (U.S. Geological Survey, 2017), as the volume of wastewater injected into the subsurface has declined owing to regulatory action and economic forces (Roach, 2018).

In Oklahoma, the rate of seismicity dramatically increased from 2009 to 2015, in some years exceeding that of California. Earthquakes owing to both wastewater disposal and hydraulic fracturing increased the earthquake hazard in these areas (Skoumal and others, 2018; Skoumal and others, 2020). During that period, Oklahoma experienced four earthquakes of $M \geq 5$, namely the $M5.7$ Prague earthquake in 2011, and the $M5.1$ Fairview, $M5.8$ Pawnee, and $M5.0$ Cushing earthquakes in 2016 (U.S. Geological Survey, 2017). Shaking from $M \geq 5$ earthquakes caused considerable damage to local buildings and infrastructure (Delatte and Greer, 2018). Oil and gas operations stopped expanding in 2015 in the parts of Oklahoma with the highest induced earthquake rates, in part to reduce the potential for induced seismicity (Boak, 2016). Starting in 2016, hydraulic-fracturing-related seismicity increased in the South-Central Oklahoma Oil Province and Sooner Trend of the Anadarko Basin in Canadian and Kingfisher counties plays in southeastern Oklahoma.

Seismicity rates subsequently increased in parts of Texas and New Mexico, as the scale of operations in the Permian Basin expanded. In 2020, a $M5.0$ earthquake occurred within the Permian Basin (Skoumal and others, 2021b) followed in late 2022 by $M5.2$ and $M5.4$

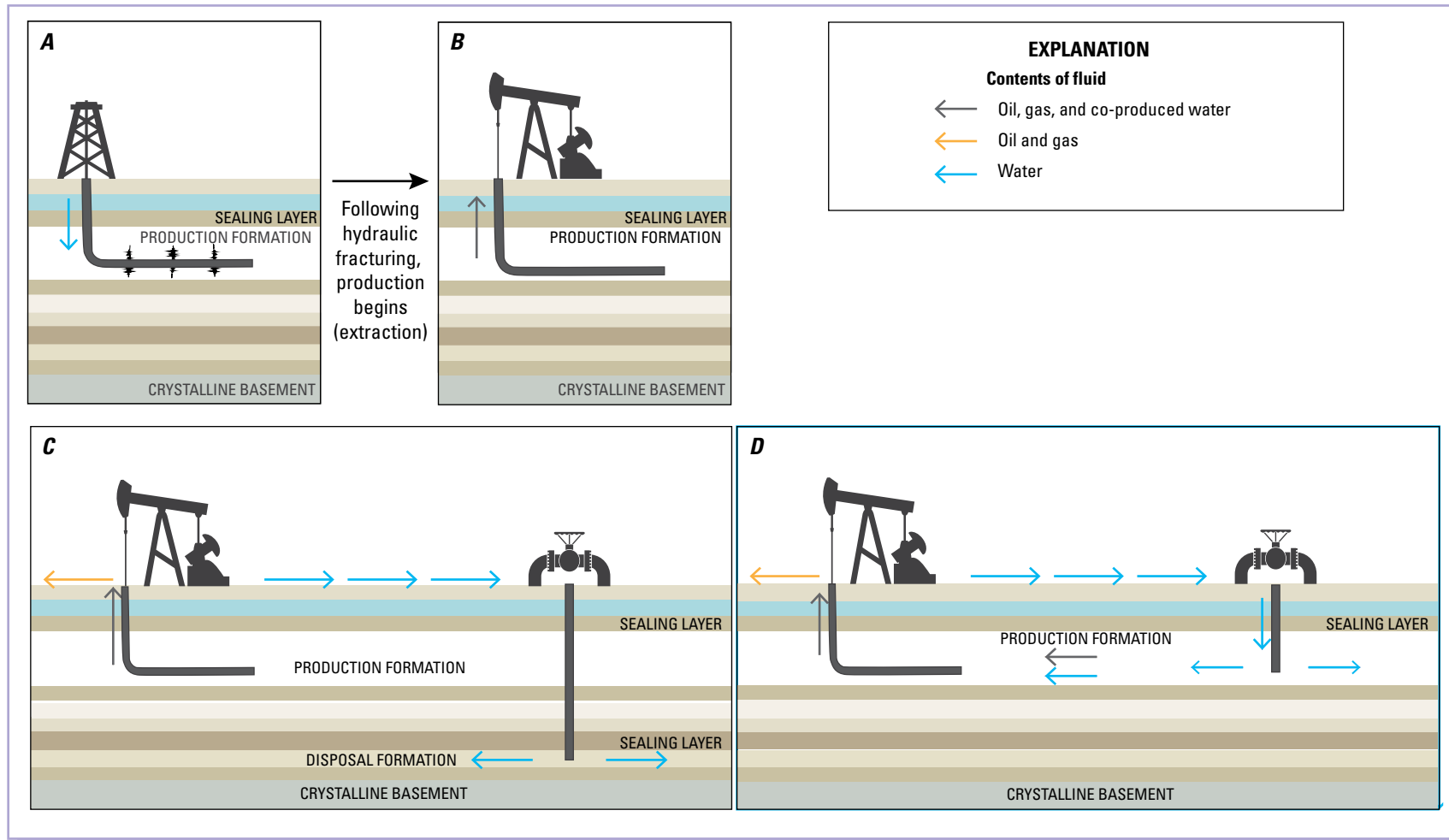


Figure 2. Simplified diagrams of oil-field operations. The geology in these diagrams is simplified from natural situations in which many more rock layers are present. Arrows show the directions of fluid being injected or withdrawn. *A*, Diagram showing hydraulic fracturing of a production well undergoing high-pressure injection for a period of hours to days. The high pressures fracture the rock surrounding the well and increase permeability. Increased permeability allows for the extraction of oil or gas from a larger region. This technique of high-pressure injection is known as hydraulic fracturing (fracking). Following the hydraulic fracturing of a well, the well goes into production. *B*, Production wells extract oil and gas from the ground. Some, but not all, production wells are hydraulically fractured. *C*, Production wells extract oil and gas and, as a byproduct, salt water. The salt water is found in the same formation as the oil and gas and is commonly termed “produced water.” The oil and gas are separated from the produced water, and the produced water is injected into a different formation using a disposal well. In practice, the wastewater from many production wells is injected into a single injection well. *D*, An alternative to wastewater disposal is enhanced oil recovery. In enhanced oil recovery, produced water is injected into the formation holding the oil and gas. The injection of produced water is intended to sweep oil and gas that is close to the injector toward the production wells to enhance oil recovery. Modified from Rubinstein and Mahani (2015).

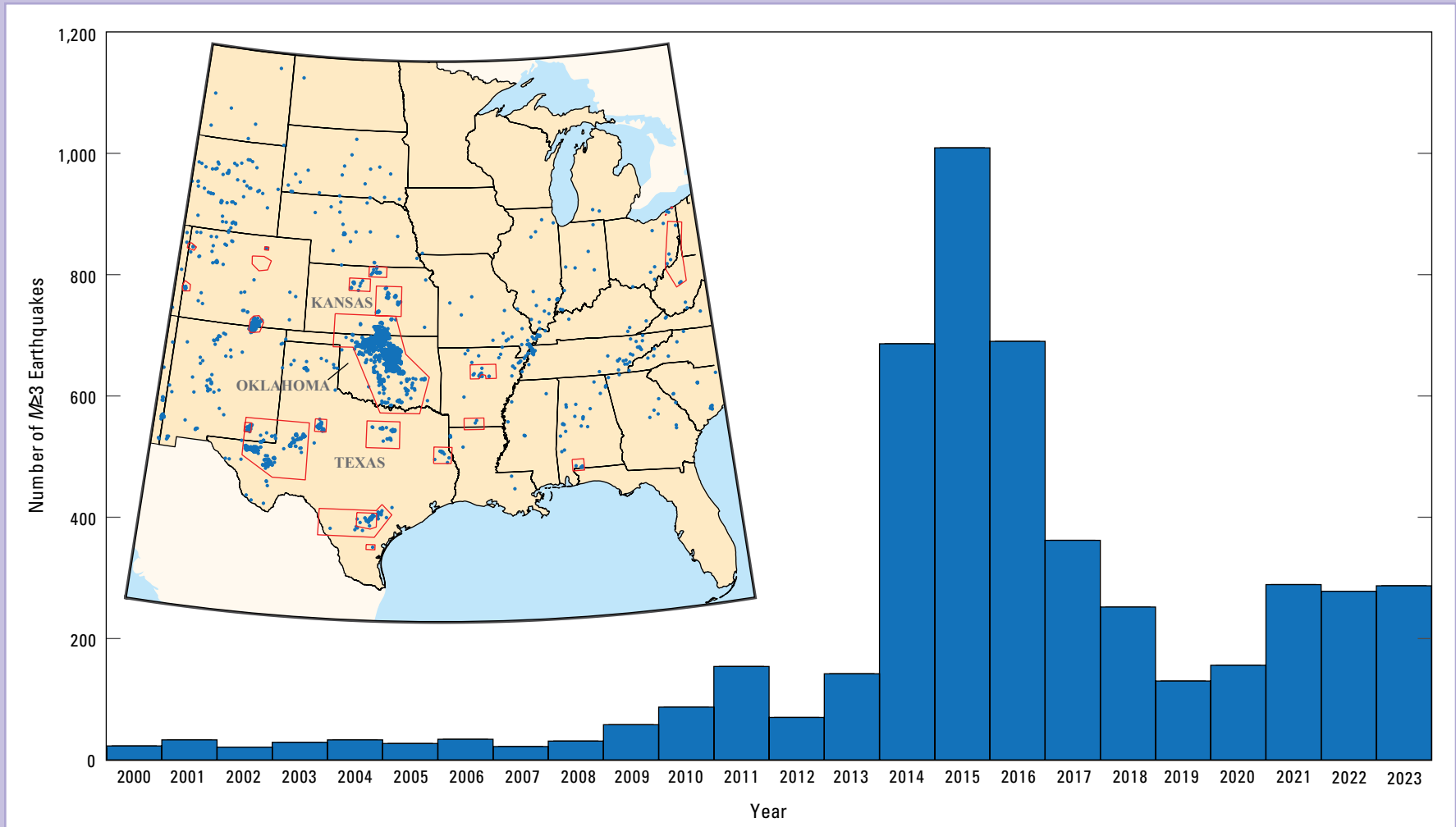


Figure 3. Rate of magnitude (M) ≥ 3 earthquakes in the central United States from 2000 to 2023 (U.S. Geological Survey, 2017). Inset shows a map of the earthquake locations with areas of likely induced earthquakes outlined by red polygons. Earthquake rates peaked in 2015, primarily owing to wastewater disposal-induced earthquakes in Oklahoma and southern Kansas. Increased rates since 2021 were primarily due to expanding oil and gas production in the Permian Basin in west Texas (for example, Skoumal and others, 2020; Skoumal and others, 2021b).

earthquakes and a $M5.2$ in 2023; these are some of the largest injection-induced earthquakes on record, albeit smaller than the largest injection-induced earthquakes ($M5.7$, $M5.8$) that have occurred in Oklahoma (U.S. Geological Survey, 2017). Texas oil production has grown by more than 300 percent since 2010, and it is the largest producer of crude oil in the United States (U.S. Energy Information Administration, 2022c). Rate forecasts indicate a prolonged period of elevated seismicity rates in the Permian Basin, even with some hypothetical mitigation strategies (Skoumal and others, 2021b).

Geothermal

Geothermal energy production involves the injection and withdrawal of fluid and carries the potential for increased hazard from induced earthquakes. Geothermal energy is one of the major renewable energy sources of electricity in the United States. For example, geothermal sources represent nearly 10 percent of Nevada's total state electricity generation, and nearly 6 percent of California's total electricity generation (U.S. Energy Information Administration, 2022a, 2022b).

In general, geothermal technologies rely on circulating large volumes of brine (or steam) transported from deep within the reservoir, through heat exchangers at the surface, and subsequently back into the reservoir (Sharmin and others, 2023). For thermodynamic and industrial engineering reasons, a measurable proportion of fluid can be lost during this cycle of production and injection (Brown and others, 1999). Such losses cause, in nearly all known instances, a gradual decline in reservoir pressure, in addition to a reduction in reservoir temperature and significant surface deformation that is detectable by geodetic methods (for example, Barbour and others, 2016; Eneva and others, 2018; Materna and others, 2022). Surface deformation is particularly costly in regions with low tolerance to pronounced changes in grading, such as agricultural regions that depend on precise leveling for flood irrigation, or population centers (Viets and others, 1979). Induced ground deformation and seismicity at geothermal fields are not mutually exclusive though; induced seismicity

is a common phenomenon at natural and engineered geothermal systems (EGS) owing, in large part, to the process of fluid production and re-injection (Barbour, 2021).

Natural geothermal systems are often located in regions with high crustal strain rates and high natural seismicity; the largest producing fields in the United States are located within transition zones of major, active fault systems such as the San Andreas Fault (fig. 4). Consequently, isolating the fingerprint of induced seismicity in regions of high natural seismicity is a challenging task (Schoenball and others, 2015; Barbour, 2021), and several fundamental, outstanding questions remain about the interactions among fault slip rates, fault-to-fault interaction, and earthquake recurrence—essential ingredients of seismic-hazard assessment (for example, Petersen and others, 2015). Further, it is not clear how assessments of seismic hazard in these regions might be biased by geothermal activities, especially if geodetic data are used to constrain fault-slip rates without considering anthropogenic effects (Barbour, 2021).

Much of the increase in geothermal production that is required to meet the growing need for clean energy sources will likely be fulfilled through EGS (Ziagos and others, 2013). EGS relies on enhanced permeability between injection and production well pairs to improve the efficiency of heat transfer, which is achieved by initially injecting fluid at high pressure into the low-permeability formations to create new fracture pathways and increase the aperture of existing pathways. The renewed focus on EGS technologies has given rise to new challenges in mitigating induced seismicity above nuisance levels (events felt but no damage occurs). Some mitigation has been successful (see Kwaitek and others, 2019), whereas some has not (see Kim and others, 2018; Woo and others, 2019).

When developing EGS, the temporal and spatial evolution of seismicity is used to track the progress of hydraulic stimulations, but the conditions that prevent small, induced earthquakes from turning into large, destructive ones are not well understood. Careful measurement of in situ conditions may provide information to mitigate the hazards of moderate earthquakes, and provide a more thorough understanding of the underlying physical processes that govern the causative relationships

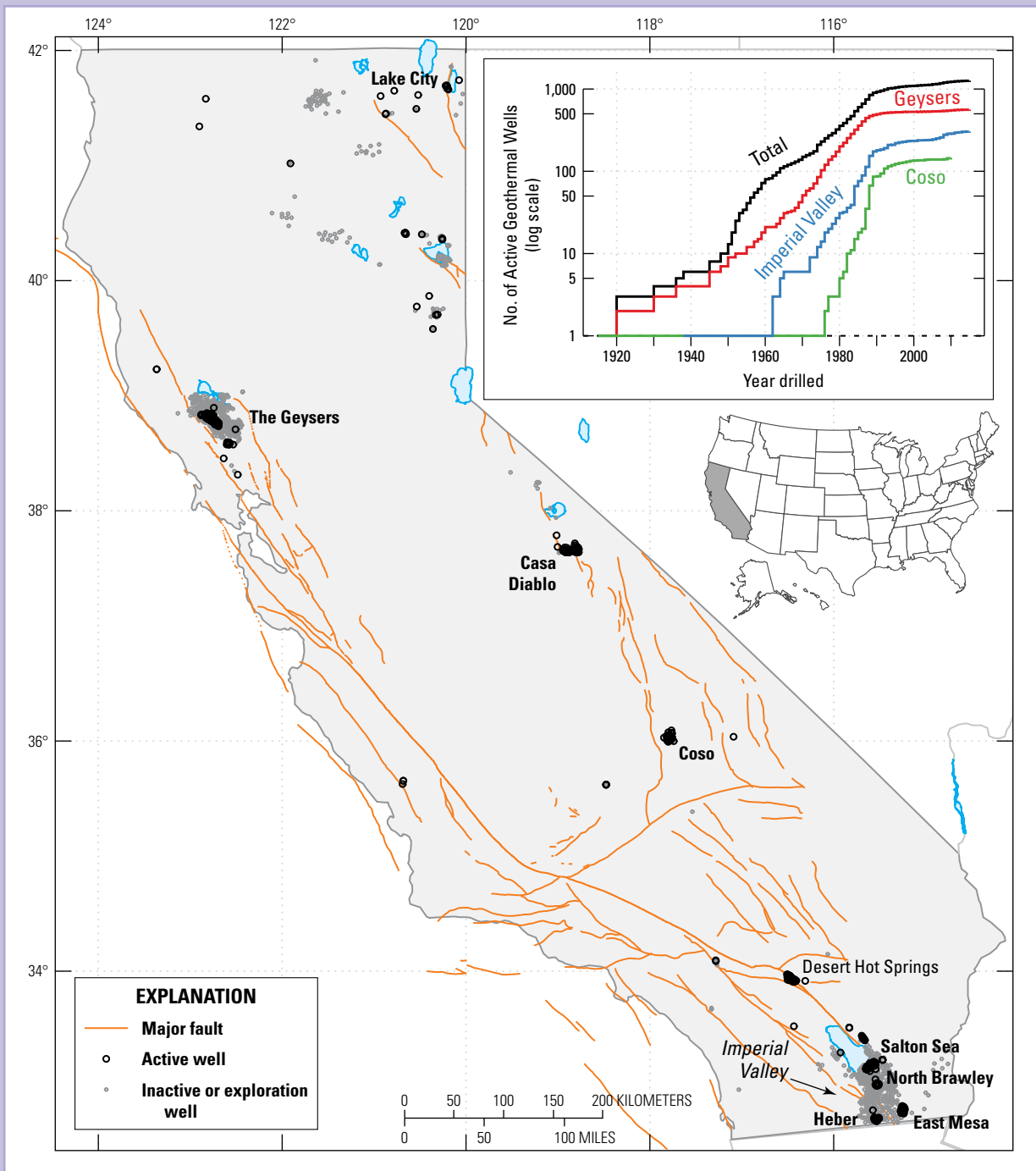


Figure 4. Map showing locations of geothermal wells and major faults in California. Inset map shows the total number of wells throughout time, broken out by major energy-producing fields—namely The Geysers; Coso; and the Imperial Valley, which includes the Salton Sea, North Brawley, Heber, East Mesa geothermal fields. Data are from the California Department of Conservation (2023). Abbreviation: no., number.

between injection and small- and moderate-magnitude seismicity in geothermal reservoirs. To address these gaps in understanding, we employ an integrated approach that involves borehole stress and geomechanical measurements, laboratory testing of recovered core samples, precision earthquake relocations, seismic velocity and geologic structure refinement, and thermal-hydrological-mechanical modeling.

Geologic CO₂ Sequestration

Geologic CO₂ sequestration (GCS) facilitates the capture and long-term storage of CO₂ (for example, Klara and others, 2003; Benson and Cole, 2008; Newell and Ilgen, 2019), a greenhouse gas contributing to climate change. Large point source emitters, such as corn ethanol plants, are a focus of CO₂ capture and storage (Sanchez and others, 2018). The GCS process involves injection of supercritical, fluid-form CO₂ into the subsurface where it is trapped within the pore space of rocks overlain by low permeability formations and (or) precipitation of carbonate minerals using the injected CO₂, a process called mineral trapping (Newell and Ilgen, 2019). The introduction of CO₂ into the subsurface adds mass and increases the pore pressure of the storage formations, which have the potential to induce earthquakes (Zoback and Gorlick, 2012; Kaven and others, 2015b; White and Foxall, 2016). These induced earthquakes pose shaking hazards to nearby populations and represent a threat to the integrity of the natural sealing formation, which may allow for the escape of CO₂ into overlying formations or back into the atmosphere (Zoback and Gorlick, 2012).

Promising conditions for widespread application of GCS are found in deep saline formations, such as those found throughout the central United States, as well as California's Central Valley (fig. 5). One such site is the Illinois Basin, which has seen the most substantial research and development of GCS in the United States. Specifically, at Decatur, Illinois, the Department of Energy (DOE)-supported Illinois Basin Decatur Project (IBDP) and the Illinois Industrial Carbon Capture and Storage Project (ICCS) utilize CO₂ from a corn-ethanol plant (Greenberg and others, 2018). Injection for the IBDP began in 2012, and roughly one million metric tons of supercritical CO₂ was injected over three years (Kaven and others, 2015b). The ICCS project started in June 2015 and has since been injecting CO₂ at nearly 1 million metric tons per year (Sanchez and others, 2018).

The ISP has been monitoring microseismicity at the Decatur, Ill., GCS site using a dedicated seismic network since 2013 (Kaven and others, 2014b; Kaven and others, 2015b). Induced earthquakes at this site have been small so far, but even small earthquakes could damage the natural sealing formation(s), which could allow escape of CO₂ back into the atmosphere. Additionally, the physical processes at play and the geologic setting of the Illinois Basin site are not unlike wastewater injection sites across the central United States; the potential for larger, felt earthquakes that could possibly damage surface infrastructure merits careful evaluation. Thus, understanding the physical processes at play and how they differ from wastewater injection is important to understand the seismic hazard that widespread adoption of GCS might pose, and to develop mitigation strategies for the occurrence of induced earthquakes in GCS.

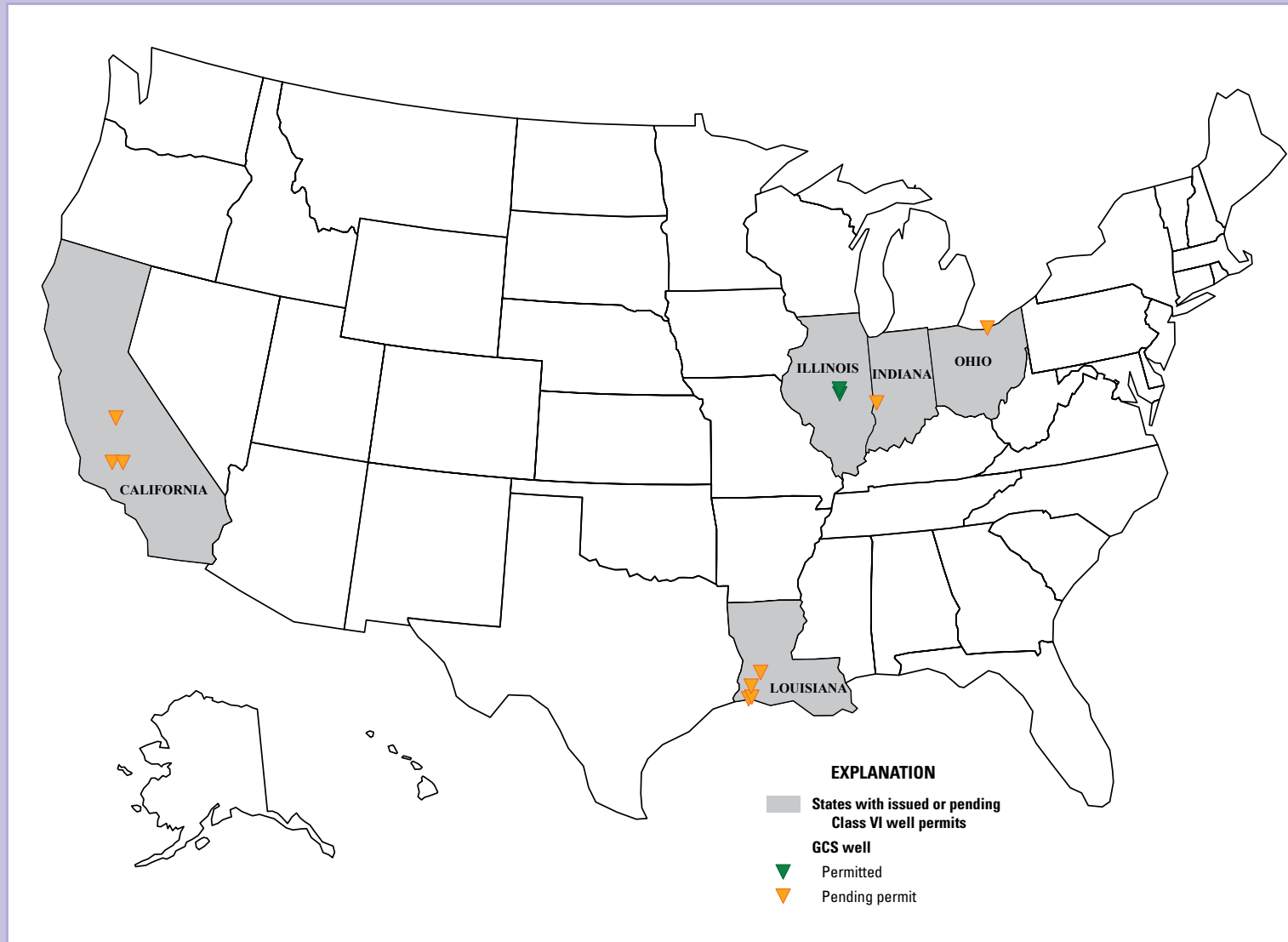


Figure 5. Locations of current and pending permits for geologic CO₂ sequestration (GCS) wells (Class VI wells) in the United States (U.S. Environmental Protection Agency, 2022).

Broader Partnerships and Communication

The USGS is dedicated to understanding the conditions that lead to induced seismicity, mitigating the associated hazards, and assisting the Nation in meeting its future needs in energy production and mitigation of climate change. Toward this goal, members of the ISP partner with other Federal and State agencies, such as the USGS Energy Resources Program, USGS Water Science Centers, DOE, the U.S. Environmental Protection Agency (EPA), national laboratories, the Oklahoma Geological Survey, the Kansas Geological Survey, the Illinois State Geological Survey, New Mexico Bureau of Geology and Mineral Resources, and the Texas Bureau of Economic Geology, among others to monitor earthquakes and investigate potential instances of induced seismicity. The DOE, in particular, recognizes the hazards posed by induced seismicity to ongoing oil and gas production, future expansion of geothermal energy in the United States, and the geologic sequestration of CO₂. The DOE has funded a considerable amount of work in this area through the USGS, the national labs, state geological surveys, U.S. universities, and private industry. We also partner with researchers at U.S. and international universities and institutions on studies relevant to ISP priorities.

Information about induced seismicity activity and research findings is provided to external partners, such as the DOE, EPA, Bureau of Land Management, U.S. Navy, New Mexico Land Trust, Texas Railroad Commission, Colorado Oil and Gas Conservation Commission, Oklahoma Corporation Commission, Kansas Corporation Commission, Kansas Department of Health and Environment, New Mexico Energy, Minerals and Natural Resources Department, Wyoming Department of Environmental Quality, California Department of Conservation, California Earthquake Authority, California Energy Commission, California Geological Survey, as well as the public. Outreach activities consist of publication of research findings; talks at scientific and engineering meetings and university seminars; presentations and briefings to governmental agencies, tribal nations, private industry, and civic groups; participation in advisory groups and review or planning committees; as well as development of fact sheets and webpages. ISP staff regularly participate in media interviews or lead press releases to provide information about recent earthquake activity that is potentially induced and to report research findings. Public lectures on induced earthquakes are given at informal and formal learning centers (schools, museums, and so on).

Prioritized Areas for Advancements

Many of the strategies and approaches to investigating and understanding induced seismicity are shared across the three task areas (oil and gas, geothermal, and CO₂ sequestration). The current capabilities and prioritized work in six key topical areas are described below: (1) seismic monitoring and analysis, (2) geodetic monitoring and analysis, (3) geophysical studies of geologic structure and physical properties, (4) laboratory rock mechanics experiments and analysis, (5) geomechanical and hydrological monitoring and models, and (6) assessment of seismic hazard. Two emerging focus areas are also of interest for prioritization: the Permian Basin and the Frontier Observatory for Research in Geothermal Energy (FORGE) Utah. Data collection, with an emphasis on the collection of ephemeral data via monitoring efforts, in these topical and emerging focus areas during the next 5 years to address may support the following overarching research questions:

- How can seismicity that is induced by industrial activities be better distinguished from natural processes, particularly in regions with higher rates of natural seismicity?
- Can faults that may be at increased hazard for induced seismicity be identified on the basis of existing fault structures, past earthquake activity, local stress conditions, or other information?
- What geologic and operational conditions control the occurrence, spatial and temporal evolution, maximum magnitude, ground shaking, and other characteristics of induced seismic sequences?
- What roles do surface and subsurface deformation, aseismic slip, and other processes play in the occurrence of injection-induced earthquakes?
- How can induced seismicity be better forecasted to manage earthquake hazards while supporting the Nation's energy production and climate mitigation needs?

Seismic Monitoring and Analysis

Earthquake Monitoring

A high-quality earthquake catalog is fundamental to any study of seismicity. Development of an earthquake catalog requires dense instrumentation, high quality crustal velocity models, and the ability to characterize seismicity at a relatively rapid pace. ISP staff often rely on detections from the National Earthquake Information Center (NEIC) or Advanced National Seismic System (ANSS) partner networks to identify new areas of potentially induced seismicity (U.S. Geological Survey, 2017). Upon identification of an area of interest, to monitor the induced seismicity, the USGS, in collaboration with relevant partners (such as state geologic surveys):

1. determines when a rapid deployment of seismometers is needed for improved monitoring of an area of developing or evolving induced seismicity and
2. identifies locations for deeper scientific study, where local seismic networks of, for example, 10 to 20 stations within 50 to 100 km of the earthquakes are deployed on years-long timescales (for example, Rubinstein and others, 2018) or dense arrays of hundreds or thousands of nodal seismometers are deployed for short, intensive studies (for example, Dougherty and others, 2019).

The oil and gas task of the ISP maintains 20 paired seismometers and accelerometers and an additional 11 independent accelerometers for a total of 31 stations that can be deployed at one time. The ISP maintains modems, such that all data can be streamed in real-time to USGS servers. Waveform data are archived by the Seismological Facility for the Advancement of Geoscience (SAGE, formerly Incorporated Research Institutions for Seismology) and made available in real time (Seismological Facility for the Advancement of Geoscience, 2024). NEIC and regional networks use data from the ISP's stations in their routine earthquake monitoring. These instruments are used for both USGS-led deployments and occasionally loaned to partner organizations for short-term deployments in areas of interest. Easy-to-install nodal seismometers are also available and ideal for short-term, focused experiments that do not require real-time data telemetry.

The CO₂ task of ISP maintains the seismic network at Decatur, Ill., consisting of shallow borehole seismometers, surface broadband seismometers, and surface accelerometers. In addition to the USGS instruments, continuous data are recorded by two deep-borehole geophone arrays operated by research partners (Archer-Daniels-Midland and Schlumberger) and distributed acoustic-sensing data (in other words, strain rate) are recorded on fiber-optic cables. These data are all combined to monitor microseismicity more accurately at the site (Kaven and others, 2014b; Kaven and others, 2015b).

Focusing on smaller areas than is typical for regional seismic networks allows for processing a greater proportion of small ($M < 3$) earthquakes, which locally reduces the magnitudes of completeness, or the minimum magnitude above which all earthquakes in a certain region are reliably detected (Habermann, 1983). In these areas, a local velocity model is often determined using the recorded earthquakes, which allows for substantially more accurate earthquake locations, particularly depth

locations, which are critical for understanding induced seismicity. Routine, automatic processing (including phase picking and association, initial location, and magnitude) is completed using ANSS Quake Monitoring System (AQMS), which is the same software underlying the Northern California Seismic Network and many of the regional seismic networks in the ANSS (Hartog and others, 2020). Refined locations are typically determined through manual analysis. In some instances, the manually analyzed earthquake catalogs become the catalog of record, specifically the ANSS Comprehensive Earthquake Catalog (U.S. Geological Survey, 2017), which is often the basis for any future USGS (or other academic) study of induced seismicity in each region.

The ISP and its partners have maintained temporary seismic networks, developed local velocity models, and produced routine earthquake catalogs to monitor induced seismicity at selected locations. Continued monitoring of hydraulic fracturing and injection-induced seismicity in the Permian Basin and the CO₂ sequestration site in Decatur, Ill., could provide insights into the current and future earthquake hazards in those areas. Further work to monitor new areas of induced seismicity using temporary seismic arrays could support selection of locations on the basis of addressing the five overarching research questions listed in the “[Prioritized Areas for Advancements](#)” section.

Enhanced Earthquake Catalogs

Earthquake detection and location are of fundamental importance in understanding all seismicity but are particularly important for determining the specific factors that control earthquake occurrence owing to subsurface fluid injection. The standard event-detection techniques discussed in the “[Earthquake Monitoring](#)” section provide a baseline characterization of seismicity; however, new post-processing techniques can refine earthquake locations and enhance detection capability to lower magnitude thresholds, sometimes increasing the number of detected events by a factor of ten or more.

For example, at the Coso Geothermal Field in California, ISP maintains a catalog of seismicity that spans more than two decades. This high-quality catalog has been used to image the subsurface fault structures and map changes in seismic-moment release through time. Interpretations of long-term data indicate that seismicity responds to injection and production in a complicated manner involving fracture- and fault-dominated flow (Kaven and others, 2014a), as well as responding to dynamic stresses from large, regional earthquakes (Kaven, 2020).

New techniques for detecting earthquakes have been developed that include waveform correlation and subspace detections to extend earthquake catalogs to very low magnitude events (McMahon and others, 2017; Cochran and others, 2018;

Skoumal and others 2019; Cochran and others, 2020a). Techniques for improved earthquake location used by USGS seismologists may include waveform polarization, cross-correlation timing, cross-correlation stacking, double-difference earthquake relocation, and analysis of depth phases or computation of synthetics to assess earthquake depth (Li and others, 2020). New methods for earthquake detection and location are being developed at a rapid pace. These are chiefly focused on machine learning-based phase identification (Ross and others, 2019; Mousavi and others, 2020). These methods can provide more accurate seismic phase arrival times and allow for additional earthquake detections, particularly for very small magnitude earthquakes.

Streamlined earthquake detection and (re-)location methods could be achieved by implementing a machine learning-based phase picker to improve earthquake detection and location processing in real time. Thus, downstream analyses that address the fundamental research questions can begin with higher quality catalogs that require minimal or no post-processing. More rapid and precise characterization of ongoing induced-earthquake sequences could also allow for improved monitoring of the evolving hazard.

Sequence Behavior

The spatial and temporal evolution of induced earthquake sequences can be useful in understanding the primary factors that control sequence behavior. Studies look at several seismological observables, including location, number of earthquakes, inter-event times, moment rate, clustering, migration, and magnitude-frequency distributions. These observables are used to compare induced and natural sequence behavior and examined along with well-operational information (injection rates, cumulative volumes, and pressures) to better understand the physical processes that control earthquake sequences.

These studies aim, in part, to reveal how induced earthquakes might be better distinguished from natural events. For example, the relation between the spatial and temporal evolution of seismicity patterns and earthquake magnitude frequency can be examined relative to injection volumes ([fig. 6](#)) and compared to naturally occurring earthquakes (Cochran and others, 2018; Cochran and others, 2020b). In some case histories, clear correlations have been reported between seismicity and injection parameters, such as injection rates and proximity to basement (Weingarten and others, 2015; Skoumal and others, 2018; Fasola and others, 2019). Migration patterns of induced seismicity are highly variable—in some instances, apparent migration of seismicity exists (Llenos and Michael, 2013), but in others, no clear migration of seismicity is visible (Rubinstein and others, 2018).

The ISP could extend observational studies of earthquake sequence behavior to new areas of induced seismicity across different types of industries

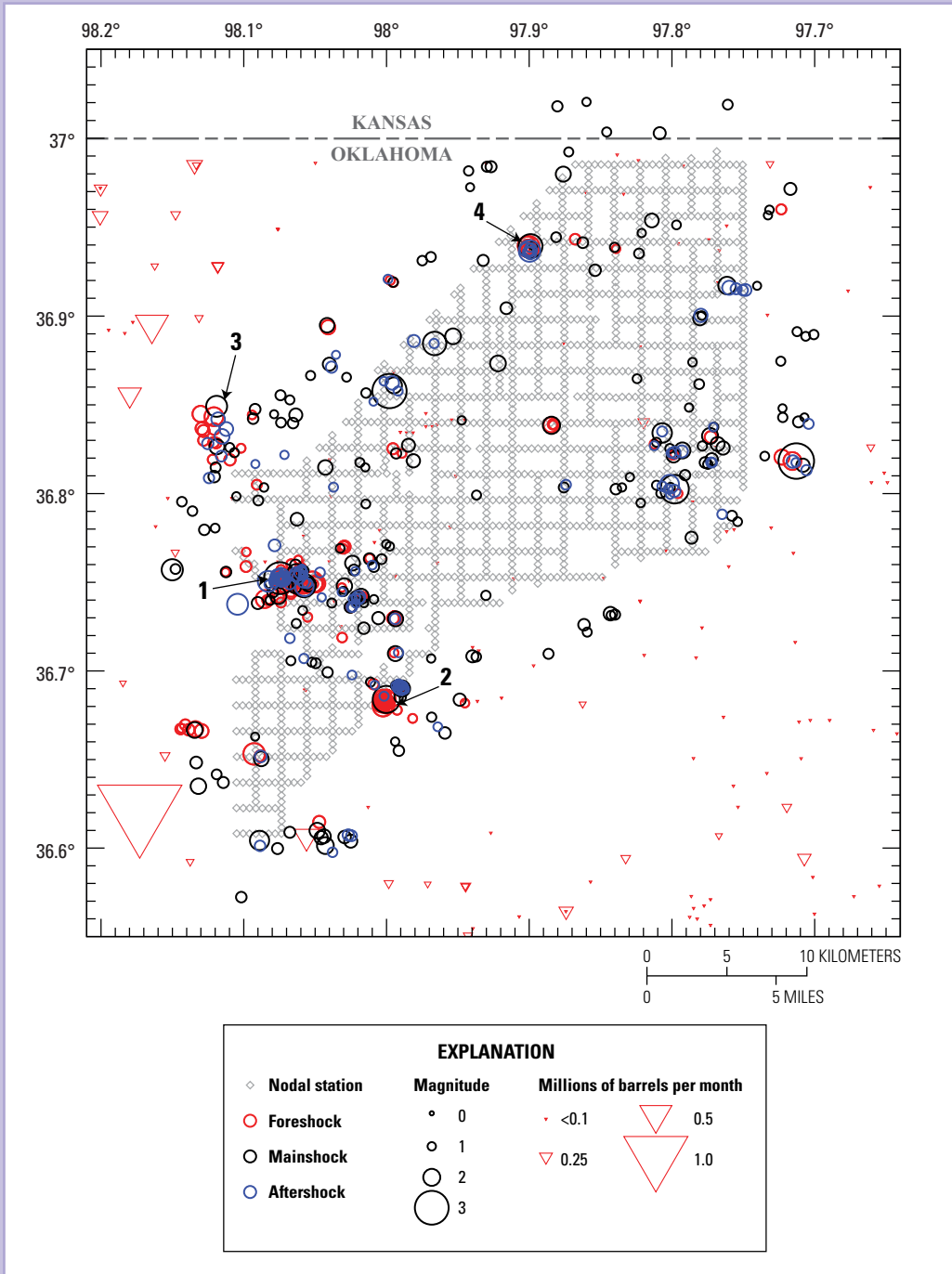


Figure 6. Distribution of foreshocks, mainshocks, and aftershocks from clustering analysis in Grant County, Oklahoma. Circles are sized by local magnitudes ranging from 0.01 to 3.0. The mainshocks for clusters with at least 10 events are highlighted and labeled (1, 2, 3, 4). The 1,829 nodal stations that comprise the Large-*n* Seismic Survey in Oklahoma array stations are shown by gray diamonds in a grid pattern. Injection well data in Oklahoma from the Oklahoma Corporation Commission (2023) scaled by average monthly volume from 2011 to 2016 are shown by red triangles ranging from less than 0.1 million barrels per month to more than 1 million barrels per month. Modified from Cochran and others (2020b).

(injection-induced, hydraulic fracturing, CO₂ sequestration, and geothermal). The ISP could also expand connections with industry partners to collect and analyze additional operational data. Modeling of induced sequences can be undertaken to determine the conditions (fault structures, preexisting stresses, pore-pressure changes) that result in various sequence behaviors (highly clustered sequences versus independent events). The ISP could continue research that explores the differences in sequence behavior between induced and natural events.

Source Properties

Source properties (for example, faulting type, stress drop, rupture history) are critical to understanding the relationship between industrial activities and seismicity, as well as for testing of seismic observations against hydrologic and geomechanical models of stress and fluid pressure changes induced by these activities. Given observations at many sites, first-motion focal mechanisms, once determined, indicate the style of faulting (Sumy and others, 2014; Rubinstein and others, 2018). In cases with few observations, composite focal mechanisms and synthetic seismograms can be used to evaluate source properties (Rubinstein and others, 2014). Full-waveform moment tensor solutions (Yeck and others, 2016) and (or) relative focal mechanisms are computed in places with sufficient station coverage (Shelly and others, 2016). Stress-drop estimates remain an area of active study (Boyd and others, 2017; Sumy and others, 2017; Trugman and others, 2017; Kemna and others, 2021; Pennington and others, 2022).

The application of new techniques (finite fault inversion of small events), collection of dense datasets (temporary deployments, including nodal arrays), and continued collaboration with academic, industry, and Federal and State partners may help refine stress-drop estimates and rupture properties of induced events. Complementary research efforts in the EHP exist that could be leveraged to explore the relationship between source properties and high frequency ground motions of induced events as well as whether source properties differ between natural and induced earthquakes.

Geodetic Monitoring and Analysis

Geodetic monitoring of ground deformation at geothermal fields has proven to be an important component in assessing causes of induced seismicity. At the Salton Sea and Coso Geothermal Fields in California, interferometric synthetic aperture radar (InSAR) observations of millimeter-scale surface displacements were used to show that the observed ground deformation there cannot be attributed solely to ongoing fault slip, either seismic or aseismic; instead, most of the observed deformation is a result of reservoir compaction associated with fluid-mass loss from geothermal operations (Barbour and others, 2016; Eneva and others, 2018). At neighboring fields in the Imperial Valley of southern California, data were used from not only advanced InSAR observations, but also data from more traditional survey methods, such as continuous and campaign global navigation satellite system (GNSS) and line-of-sight leveling to document quasistatic and transient deformation at the Heber Geothermal Field (see Barbour, 2021). At the North Brawley Geothermal Field, Materna and others (2022) further supplement these data sources with National Aeronautics and Space Administration (NASA) Uninhabited Aerial Vehicle (UAV) Synthetic Aperture Radar (SAR) to document a decade of aseismic fault slip on reservoir-bounding faults. This diverse set of geodetic data and methods has been crucial to measuring ground deformation around these fields, which operate within a region of vigorous agricultural activities.

In general, ground deformation at geothermal fields is easily detected with such geodetic methods, but signals related to wastewater injection-induced earthquakes in the central United States have been more elusive. Nonetheless, some of the larger magnitude events have generated measurable coseismic deformation that offers critical insight into rock properties and source depths (for example, Barnhart and others, 2014; Barnhart and others, 2018; Skoumal and others, 2021). In some instances, geodetic data are critical for understanding the depth distribution of slip and its relation to operation activities like hydraulic-fracturing

stimulations, especially in remote regions, where seismic data coverage is poor (for example, Wang and others, 2022). Geodetic data have also shown that deformation from wastewater disposal may not always generate seismicity (Shirzaei and others, 2016), yet another indication that aseismic effects of fluid injection may be more common than previously expected.

Geodetic data provide useful information about seismic and aseismic processes, including slip rates, moment-release budgets, and ground-deformation anomalies. In regions with high natural hazard and vigorous induced seismicity, such as the Imperial Valley, Calif., work to separate natural and anthropogenic deformation processes may continue, using observational studies complemented by advanced thermal-hydrological-mechanical modeling. New sources of geodetic data, including fiber-optic strain (for example, Utah FORGE), and the upcoming launch of the NASA-Indian Space Research Organization (ISRO) SAR (NISAR) satellite may provide improved observations of induced seismicity-related deformation.

Geophysical Studies of Geologic Structure and Physical Properties

Fault Identification from Seismicity

Most faults that host induced earthquakes are unknown until induced seismicity is observed, for example, in Oklahoma (Schoenball and Ellsworth, 2017). Knowledge of local fault structures is potentially valuable for improving hazard estimates and assessing operational decisions made by industry. The enhanced catalogs developed using the techniques described above, along with the recently developed FaultID method, can be used to delineate local fault structures and their orientations (Skoumal and others, 2019) (fig. 7). Given the incredible number of events in some induced earthquake catalogs (thousands to tens of thousands),

such automated fault identification is necessary because manually defining such high numbers of faults is intractable. At present, the FaultID method has been applied in Oklahoma (Skoumal and others, 2019; Cochran and others, 2020a) and Texas (Skoumal and others, 2021b).

FaultID or similar techniques can be applied to additional locations of induced seismicity to determine fault structure in areas of high-resolution seismicity catalogs. Further improvements to methodologies could refine the resulting fault structures and results could be compared to fault structures from other data sources.

Stress State

Another way the ISP investigates the conditions that may influence the occurrence of induced seismicity is by determining crustal stress orientations. Capabilities for measuring stress include using focal mechanisms (for example, Rubinstein and others, 2018; Skoumal and others, 2021a), moment tensors (for example, Amemoutou and others, 2021), and shear wave splitting (for example, Cochran and others, 2020a; Skoumal and others, 2021a). Most wastewater disposal-induced earthquakes align on apparent faults that are generally well oriented within the regional stress field; however, events can occur along faults that are poorly oriented within the stress field, for example, the $M4.9$ Milan, Kansas earthquake (Joubert and others, 2020) as well as the $M5.0$ Prague, Oklahoma foreshock and $M5.0$ Prague, Oklahoma aftershock (Cochran and others, 2020a). Information about the local stress field is valuable for interpreting the ongoing seismicity as well as assessing the probability of failure for known structures in a region.

In geothermal settings, the ISP has significant experience in measuring the state of stress in the crust using inversions of earthquake focal mechanisms and borehole observations (for example, borehole breakouts, injection falloff, and so on) (Hickman, 1991). In partnership with Sandia National Laboratory, the ISP

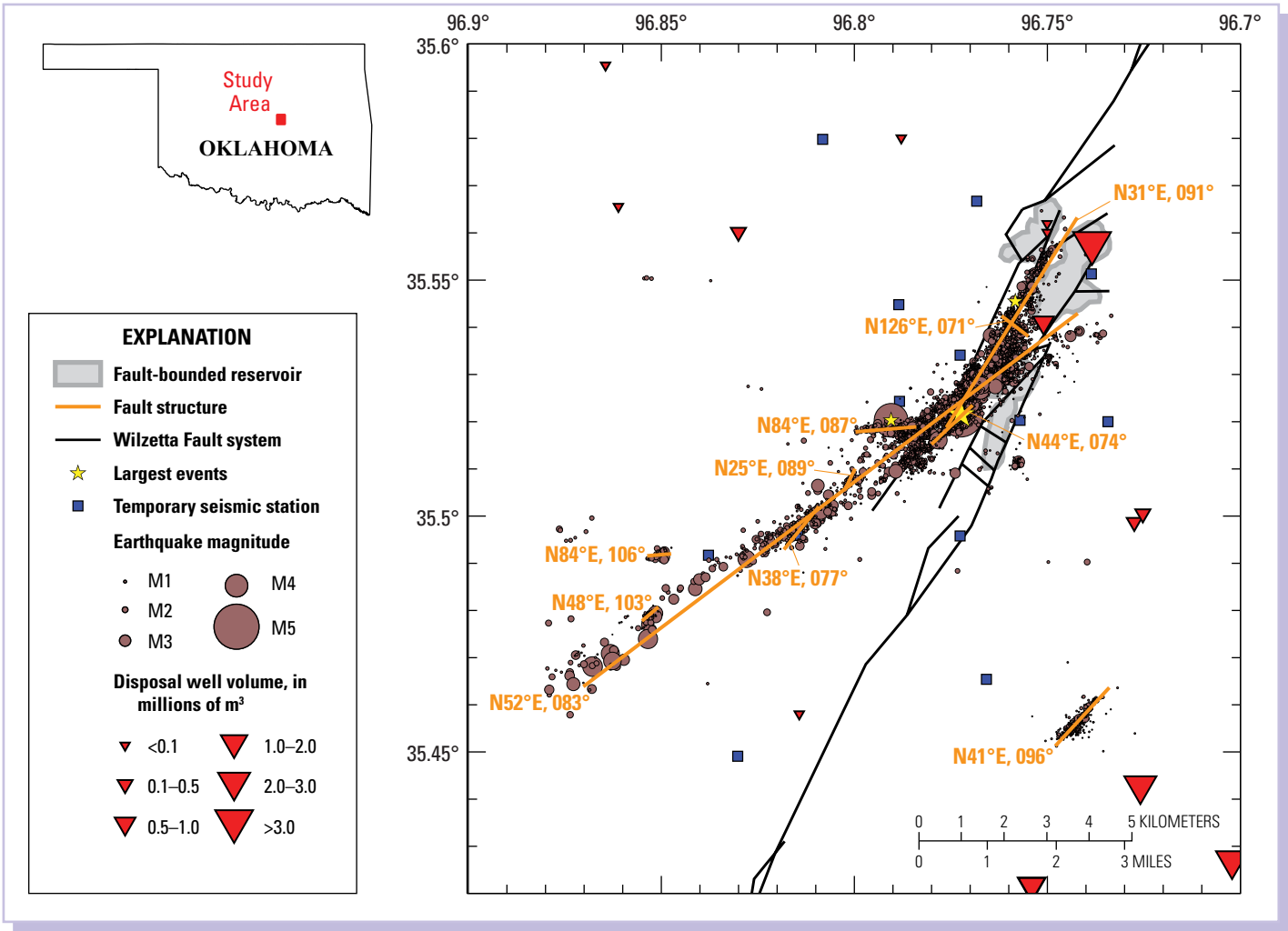


Figure 7. Fault structures (orange lines with labeled strike and dip) of the 2011 Prague, Oklahoma, earthquake sequence identified with FaultID using aftershock locations. Yellow stars indicate the locations of the three largest events in the sequence (*M*4.8 foreshock, *M*5.7 main shock, and *M*4.8 aftershock). Temporary seismic stations are shown by blue squares. The black lines show the Wilzetta Fault system based on regional and local seismic and geological studies (Way, 1983). The red inverted triangles show wastewater disposal wells sized on the basis of the volume of fluid injection during their lifetime of operation until the end of 2010 into fault-bounded reservoirs (gray shaded areas). Modified from Cochran and others (2020a). Abbreviation: *M*, magnitude.

uses an acoustic televiewer designed for operation in high-temperature boreholes, under conditions that traditional equipment would typically fail, to image breakouts and other stress indicators. These and other borehole data have been used to inform analyses of the in-situ state-of-stress at existing and proposed geothermal plants and EGS sites, including at Coso, Calif.; Desert Peak, Nev.; Fallon, Nev.; and Raft River, Idaho, during the DOE-funded FORGE site-selection process (U.S. Department of Energy, 2024).

Tools can be refined for estimating stress from focal mechanisms and shear wave splitting and applied to areas of ongoing and new induced seismicity. Spatial and (or) temporal variability in the local stress fields near regions of active wastewater disposal may be of interest for further study.

Laboratory Rock Mechanics Experiments and Analysis

The ISP, in collaboration with experts in rock physics, performs hydrothermal testing of faults, fractures, and fault zone materials. Tests include (1) time-dependent strength recovery and healing, (2) time-dependent permeability evolution, (3) effects of shearing on strength and permeability, (4) time-dependent velocity recovery of faults following earthquakes, akin to velocity recovery of fault zone-trapped waves, (5) influence of cementation and alteration on fault zone properties such as strength, permeability, porosity, electrical resistivity, aperture, velocity, modulus effect of deformation, and (6) time-dependent volume change and associated pore pressure change on fault stability (for example, Proctor and others, 2020).

The results from these tests are key to understanding the physical processes and the evolution of fractures that control induced seismicity, especially when paired with thermal-hydrological-mechanical-chemical (THMC) modeling. Additionally, this work can improve our understanding of the factors that influence the sustainability

and reactivation of fracture networks and eventually lead to strategies for improved EGS techniques to increase reservoir longevity.

Investigations of how permeability and strength evolve through time under different temperature and stress conditions may provide key insights into why induced earthquakes occur. Experiments could be integrated with THMC fracture models that may elucidate the relative contributions of various coupled THMC processes with respect to the enhancement or degradation of permeability and strength recovery.

Geomechanical and Hydrological Monitoring and Models

Downhole Pressure Monitoring

The ISP uses downhole pressure sensors to measure formation fluid pressure through time and characterize the hydro-mechanical response of wastewater reservoirs to changes in fluid pressure. In Oklahoma, the data from a deep Arbuckle Group reservoir monitoring well (Barbour and others, 2019) are sent via satellite telemetry to the Oklahoma-Texas Water Science Center, where the provisional data are made publicly available in near-real time via the National Water Information System (NWIS) (U.S. Geological Survey, 2016). Following quality control checks, the data may be revised and reclassified as final products on the NWIS site. This is one of the few ways in which conditions that may lead to induced seismicity are investigated by the ISP directly.

The downhole pressure data collected in Oklahoma have provided a powerful new dataset that has led to important new insights on the hydro-mechanical response and flow regimes of the Arbuckle Group. The ISP could seek data from additional sites that may allow for examination of spatial differences in response. For instance, the Arbuckle Group was considered a confined

reservoir, but the deep Arbuckle Group monitoring well showed evidence of leakage (for example, Wang and others, 2018). These data were also critical in demonstrating that the standard wisdom that poroelastic response of trapped fluids should only be sensitive to mean stress changes is not valid in the Arbuckle Group (Barbour and Beeler, 2021); rather, shear

stress and strain changes can also induce pressure responses (fig. 8). In both examples, however, outstanding questions remain about the strength of hydro-mechanical anisotropy and leakage out of the Arbuckle Group in the seismically active regions of Oklahoma, because the monitoring well is in a seismically quiet part of the state.

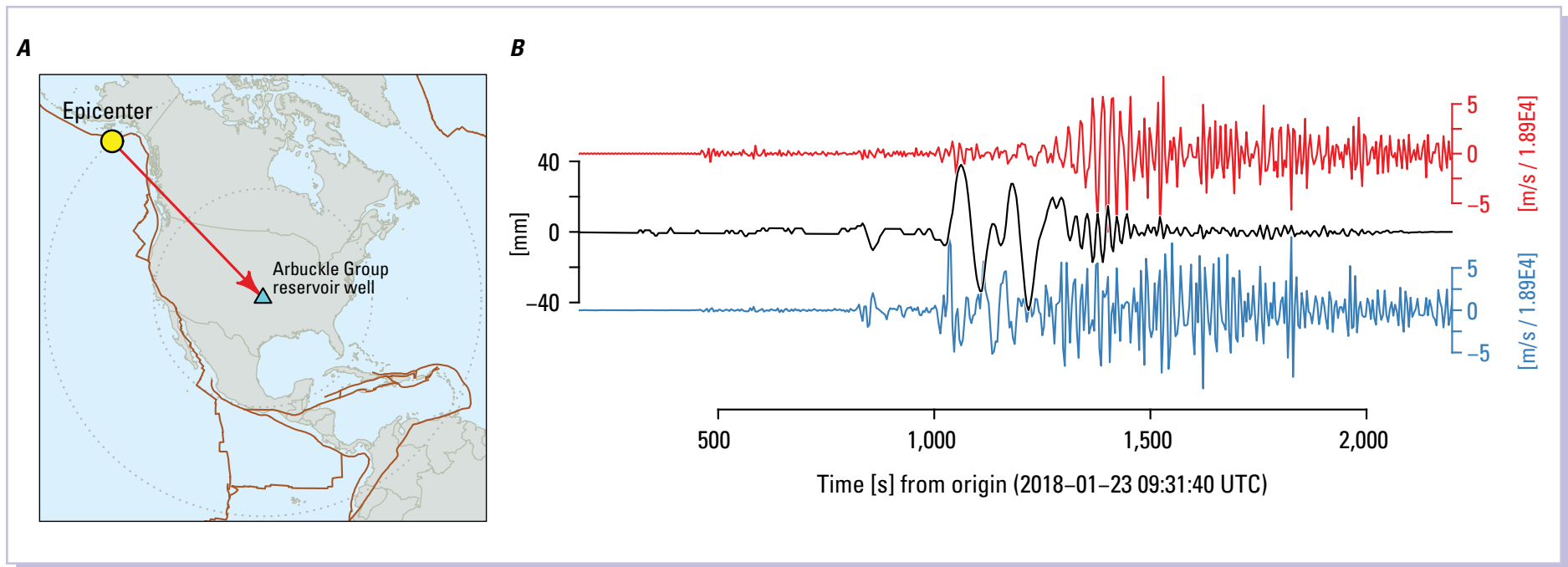


Figure 8. Map and timeseries graphs showing the shear strain response of the Arbuckle Group reservoir in Oklahoma to the 2018 moment magnitude 7.9 Kodiak, Alaska, earthquake, $\sim 40^\circ$ away. *A*, Azimuthal equidistant map of the epicenter centered on the Arbuckle Group reservoir monitoring well with plate boundary faults (dark brown lines). Dotted gray lines on map are 20-degree parallels. *B*, Timeseries, in seconds (s) from origin of event, of the fluctuations in fluid pressure (black) in the Arbuckle Group reservoir, in millimeters (mm), compared to areal (red) and shear (blue) strains, in meters per second per $1.89 \text{ E}+4$ ($\text{m/s}/1.89\text{E}4$) inferred from radial and transverse ground velocities, respectively, from the collocated broadband seismometer at the surface. Strains have been lowpass filtered to 0.25 hertz (Hz). Modified from Barbour and Beeler (2021). Abbreviations: mm, millimeters; m/s, meters per second; s, seconds

Additional pore pressure monitoring sites could be secured in states such as Oklahoma, Kansas, and (or) Texas to augment existing data for improved spatial monitoring of reservoir pressure changes. Development of a new generation of geodetic grade, fiber-optic strain sensors in collaboration with academic partners could provide new tools to aid in monitoring both seismic and aseismic fault slip as well as more distributed subsurface deformation. Additional geophysical tests (for example, active well tests) or geochemical sampling may inform understanding of reservoir leakage rates. Leakage and anisotropy analyses from regions with induced seismicity can be compared to seismically inactive regions to look for differences that could inform why seismicity occurs in some regions and not others. Strain and pressure analyses in geothermal settings may be key to understanding the complex relationship between production and seismicity.

Numerical Modeling

Numerical modeling is often necessary to understand the physics underlying induced seismicity, such as how sequences start, continue, and terminate. The ISP has the capacity to develop poroelastic, geomechanical, and hydrological models constrained by seismic, geological, and industrial data, which allow for identification of the primary drivers of seismic hazard. For instance, a simple, coupled hydro-mechanical and rate-state earthquake rupture model was developed to forecast wastewater-induced earthquake rates given injection information (Norbeck and Rubinstein, 2018). This method has been used for earthquake rate forecasts (Skoumal and others, 2021b) and hazard forecasts (Rubinstein and others, 2021). More complex modeling of the physics underpinning wastewater disposal induced seismicity has been done within the ISP but is mostly limited to case studies (for example, Barbour and others, 2017).

Geothermal fields may require more specialized modeling owing to the complex set of site-specific conditions related to reservoir temperature and pressure, as well as natural faulting and tectonic strain. At Coso, we used a coupled finite element model (FEM) of the reservoir

to understand seismic observations, which indicate that pore pressure and reservoir temperature changes in a homogeneous reservoir do not adequately explain seismic energy release. Instead, fault- and fracture-hosted flow of fluids and heat likely dominate the resultant deformation mechanisms (Kaven and others, 2015a). Some modeling results have shown that the evolution of seismicity depends on poro- and thermo-elastic stresses and their interaction with the fault structure in a complex manner. At the Heber Geothermal Field in southern California (fig. 4), crustal scale faults are the main source of hydrothermal supply, and both transient ground deformation signals and seismicity rate changes were observed in response to rapid decreases and increases in operational flow rates.

Methods used for producing wastewater disposal-related induced seismicity hazard forecasts could be modified in collaboration with earthquake forecasting experts in the USGS to include different types of fluid-injection induced seismicity including hydraulic fracturing, EGS systems, and GCS. Further, detailed FEMs could improve understanding of the interactions between operational flow rates, ground deformation, and seismicity rate changes.

Assessment of Seismic Hazard

Maximum Magnitude Expectations

One significant limitation of induced seismicity hazard forecasts is the ability to accurately predict the maximum magnitude (M_{\max}) earthquake expected for a given region of operations. Multiple methods have been developed to forecast M_{\max} of induced earthquakes on the basis of injection volumes (or pressurization rate) and (or) the spatial and temporal evolution of seismicity (for example, Shapiro and Dinske, 2009; McGarr, 2014; Yeck and others, 2015; van der Elst and others, 2016; Galis and others, 2017). Debate is ongoing as to whether a cap on the M_{\max} of induced events exists that is controlled by injection volume (as suggested by McGarr, 2014) as well

as frictional properties and pre-stress conditions (Galis and others, 2017), or whether the apparent scaling between total injected volume and M_{\max} is the result of statistical undersampling of a generally low but significant probability of earthquake ruptures that could extend outside of the pressurized zone (van der Elst and others, 2016).

Several case studies follow the volume limit (McGarr and Barbour, 2017, 2018), but a particularly notable counterexample is the 2017 M5.5 Pohang, South Korea earthquake, which injured dozens of people and caused significant damage (Kim and others, 2018; Woo and others, 2019). The Pohang earthquake greatly exceeded the expected M_{\max} predicted by the competing physics-based scaling relationships (Ellsworth and others 2019); however, given the paucity of seismicity prior to initiation of the EGS project, it is unclear how effective the purely statistical method would have been as a tool for estimating the expected M_{\max} without additional information (for example, mapped faults and structure). Recent modeling using an earthquake simulator indicates that the pre-existing stress distributions on a fault may control whether a runaway rupture occurs (Kroll and Cochran, 2021).

Continued observation of induced seismicity, along with improved simulations, could identify the conditions in which the expected M_{\max} is likely to be controlled by injection volumes (pressurization rates). Refining the expected M_{\max} estimates may be attainable on a region-by-region basis given thorough knowledge of operations, as has been done for the Groningen natural gas field in the Netherlands (Zöller and Holschneider, 2016) and at the Hutubi underground gas storage facility in China (Jiang, and others, 2021). However, at present, information about ongoing wastewater-disposal operations in the United States necessary for such detailed studies is often insufficient, if not absent entirely, so greater collaboration with industrial partners could result in significant progress on these topics.

Ground Motions

Ground-motion models (GMMs) are used to predict expected ground-shaking levels that are critical for hazard forecasts. GMMs can be a significant source of uncertainty in those forecasts, so determining whether existing GMMs for natural events are sufficient for induced earthquakes is important (Petersen and others, 2016). Evaluating GMMs requires near-source (<40 km) strong motion data (McNamara and others, 2018). Assessments of needs for temporary monitoring seismic stations near areas of active induced seismicity were conducted in collaboration with local partners for new areas of induced events to determine if near-field coverage of earthquakes was sufficient for ground-motion data collection. Data from these temporary and existing regional stations could then be used to evaluate how well GMMs predict the observed ground motions.

Early evaluation of ground-motion data suggested wastewater-injection induced event ground motions were somewhat lower than predicted (Hough, 2014).

Wastewater injection-induced earthquakes have been found to have lower ground motions than tectonic events in the nearfield (10–40 km) (McNamara and others, 2018) and quantitative evaluation of multiple GMMs suggests that regionally specific models developed for induced events are necessary (McNamara and others, 2018; Moschetti and others, 2019). Differences in expected ground motions between induced and tectonic events may provide information about the state of stress around the source, or physics of the rupture itself.

Ongoing examination of existing and new datasets of induced earthquake ground motions may provide additional insights into the factors controlling ground motion of induced events. Collection and compilation of relevant regional ground motions, development of criteria relating to GMM selection (for example, Rezaeian and others, 2014), and evaluation of potential GMMs may improve short-term hazard forecasts. New or modified ground-motion models may provide improved forecasts over current methodologies.

Short-Term Earthquake Hazard Forecast Models

Induced seismicity has traditionally been removed from the standard, long-term USGS earthquake hazard forecasts owing to its rapid variation in time and space. Given the increase in seismicity observed in the central United States, the ISP, in collaboration with the National Seismic Hazard Modeling Project, developed a method to forecast induced earthquake hazard on a 1-year timescale (Petersen and others, 2015). Forecasts of induced earthquakes were subsequently made in the Central United States for 2016, 2017, and 2018 (Petersen and others, 2016, 2017, 2018). Forecasts are an important component in assessing the increased life-safety risks (Liu and others, 2019), expected earthquake insurance claims (Wetherell and Evensen, 2016), demand for state compensation funds (Konschnik, 2017), and need for new or modified regulations of the causative industrial activities (Ehrman, 2017). These were the first large-scale hazard forecasts for induced seismicity and were based solely on the preceding earthquake rates, neglecting injection information. Although the forecasts are generally sufficient for estimating hazard, they tend to be inconsistent with observed seismicity when large inflections in seismicity rates owing to changing operational practices exist (White and others, 2017; Teng and Baker, 2019; Rubinstein and others, 2021).

Since the release of these hazard forecasts, the ISP has developed a coupled hydromechanical and rate-and-state model to forecast earthquake rates from injection (Norbeck and Rubinstein, 2018). Hazard forecasts have been developed based on the Norbeck and Rubinstein (2018) model's earthquake-rate forecasts and examined the performance of those models (fig. 9) (Rubinstein and others, 2021). Others have also developed methods for forecasting induced earthquake rates that include injection data using both empirical and physical models (for example, Langenbruch and

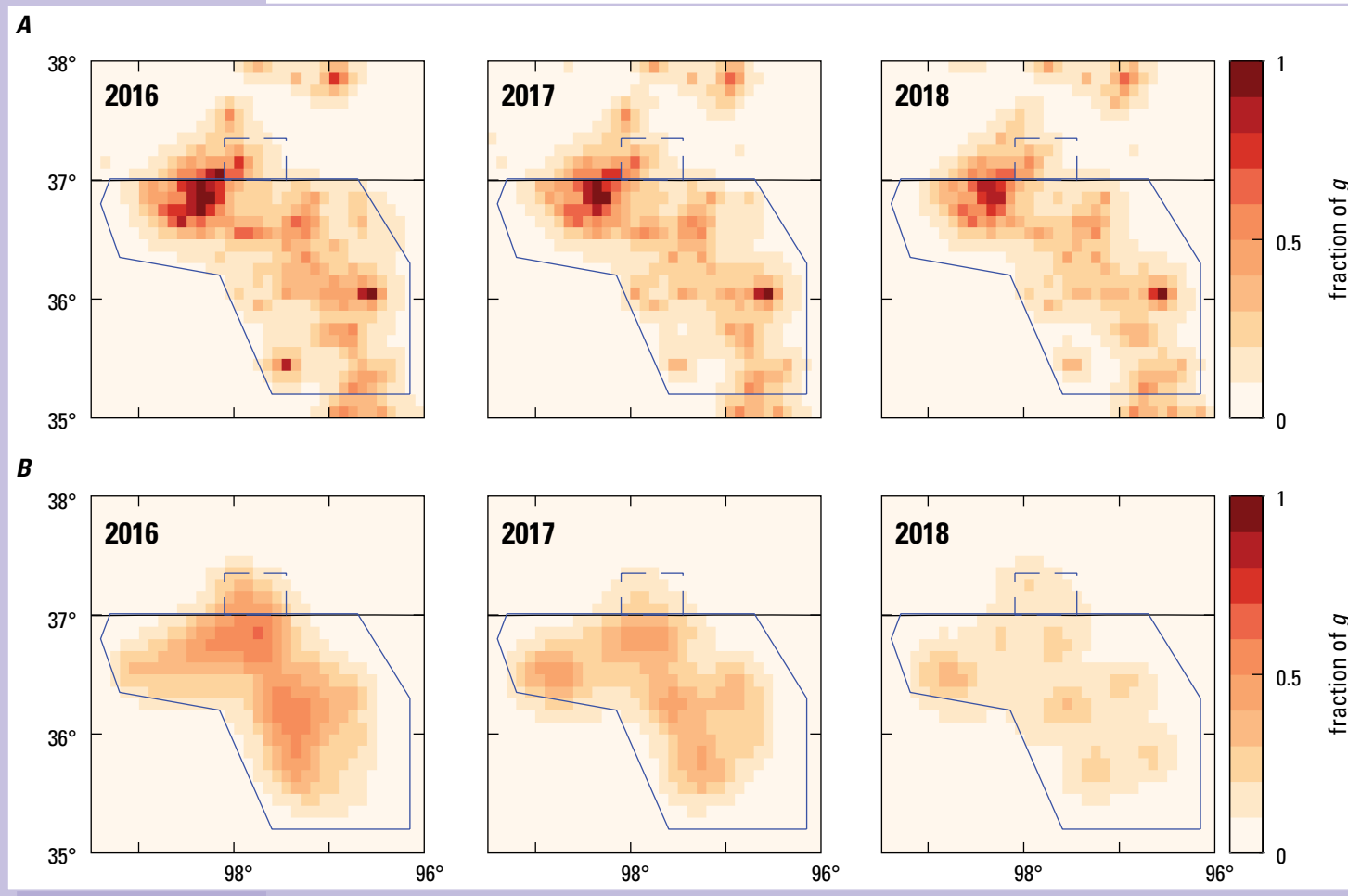


Figure 9. Comparison of peak ground accelerations (fraction of the gravity of Earth [g]) forecast in central Oklahoma and southern Kansas with 1 percent (%) probability of exceedance made by a hydromechanical model (A), observational model (B), and USGS official model (Petersen and others, 2016, 2017, 2018) (C) versus observed ground motions for all $M \geq 4$ earthquakes (D) for (left) 2016, (middle) 2017, and (right) 2018. We show results for $M \geq 4.0$ earthquakes instead of $M \geq 4.7$ because no $M \geq 4.7$ earthquakes occurred in either 2017 or 2018. Solid blue polygon shows Oklahoma area of concern and dashed blue box shows Kansas area of concern for induced seismicity. Modified from Rubinstein and others (2021). Abbreviation: M , magnitude.

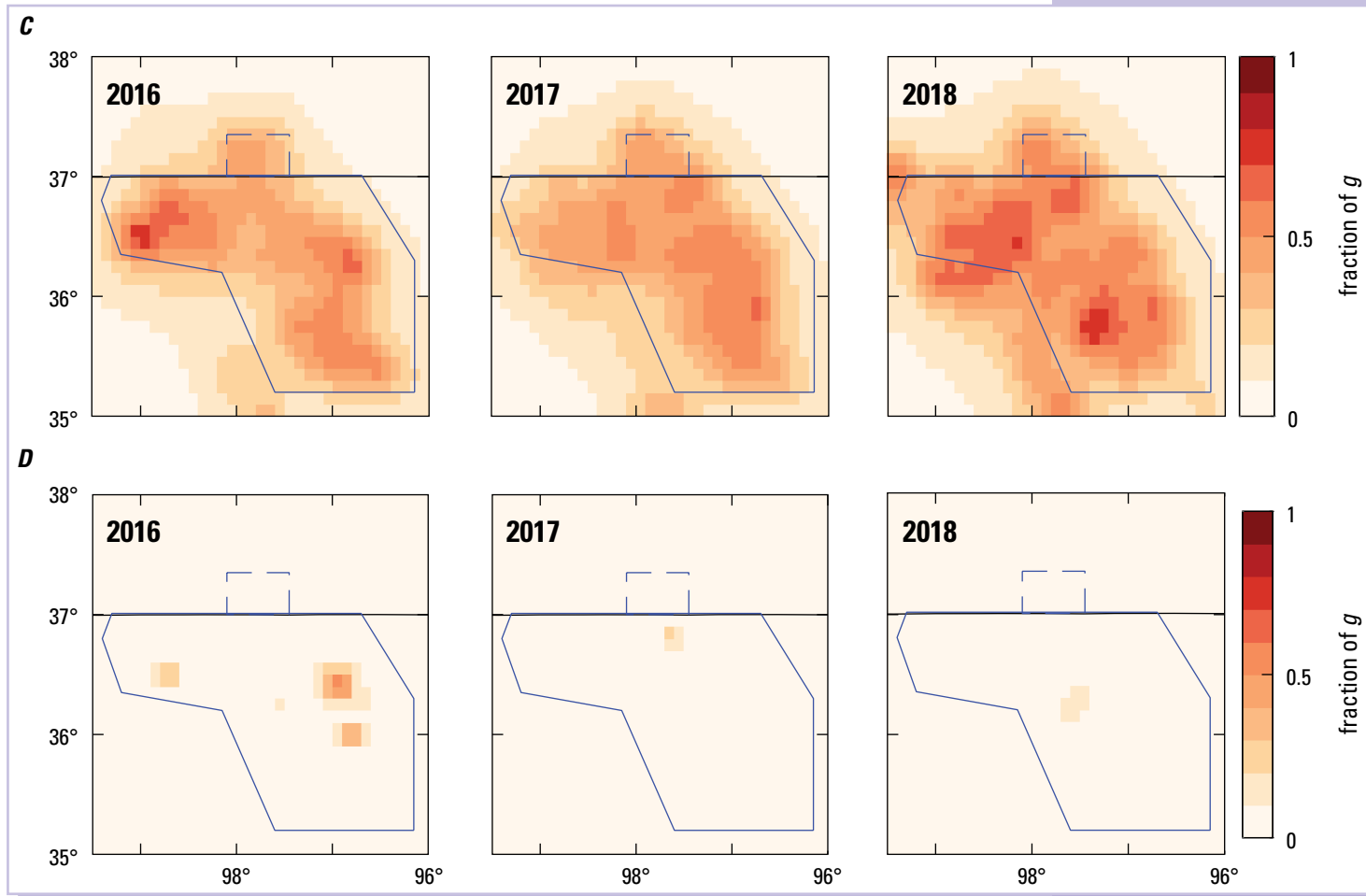


Figure 9.—Continued.

others, 2018; Dempsey and Riffault, 2019; Zhai and others, 2019; Grigoratos and others, 2020).

A hybrid approach was also developed and used both epidemic-type aftershock sequence (ETAS) modeling and changepoint detection to study the connection between changes in seismicity rate and changes in injection and production flow rates (Llenos and Michael, 2016). This approach can more accurately forecast earthquake rates that vary so rapidly that they are difficult to forecast in 1-year hazard maps, like at the Salton Sea Geothermal Field or The Geysers Geothermal Field. We additionally developed a method using a space-time ETAS model to estimate background earthquake rates in areas of wastewater-induced seismicity. This method produces declustered earthquake catalogs with properties that are consistent with the full earthquake catalog and provides uncertainty estimates (Llenos and Michael, 2020).

Although overall seismicity rates have slowed and the desire for induced seismicity hazard forecasts has declined, the growing seismicity rate in the Delaware Basin (within the Permian Basin, west Texas) suggests the possibility that future hazard forecasts may be required. At present, the physics-based forecasting methods rely on up-to-date injection data to make accurate forecasts. The variability of the availability and ease of access to injection data may pose a significant limitation to applying these methods in real time. Thus, continued research into physics-based forecast methods for both wastewater injection and hydraulic fracturing-related seismicity may improve real time applications. This includes how to appropriately handle incomplete industry data in physics-based forecasts, with an eye towards near real-time forecasts.

The USGS has developed statistical methods for Operational Aftershock Forecasts in which earthquake rates are forecast during periods of the intense seismic activity following a large earthquake or during earthquake swarms (Llenos and van der Elst, 2019; Michael and others, 2019).

This methodology may improve forecasts for induced and natural earthquake swarms, which often have brief, intense periods of seismicity. Short-term earthquake-rate forecasts could be evaluated to compare to current 1-year hazard models to determine the relative merits of each approach for forecasting induced seismicity. The operationalizing of both physics-based hazard forecasts and short-term earthquake-rate forecasts are discussed in the “[Limitations](#)” and “[Opportunities for Innovation](#)” sections.

Emerging Focus Areas

Permian Basin

The rate of seismicity in Oklahoma has decreased since its peak in 2015, whereas the seismicity rate in the Permian Basin (western Texas and southeastern New Mexico) has been increasing since 2014 ([fig. 10](#)). The rate of seismicity has increased from an average of 1 $M \geq 3$ earthquake per year to a peak of 81 $M \geq 3$ earthquakes in 2020, 188 $M \geq 3$ earthquakes in 2021, and 214 $M \geq 3$ earthquakes in 2022 (U.S. Geological Survey, 2017). The largest earthquakes in this period were a $M 5.0$ near Mentone, Texas in March 2020, a $M 5.4$ near Colson Draw, Texas in November 2022, and a $M 5.2$ near Range Hill, Texas in December 2022. Most of the seismicity is occurring in the Delaware Basin, a subbasin that makes up the western half of the Permian Basin. The majority of seismicity to date has occurred in the Delaware Basin. Routine seismic monitoring is administered by TexNet (University of Texas, 2024) in the Texas part of the basin and the New Mexico part of the basin falls within USGS purview.

In May 2021, a seismic network was fully deployed to monitor active oil and gas operations in the Permian Basin in a part of southeastern New Mexico. Continuous waveform data are streamed to SAGE and used by the NEIC, TexNet, and the New Mexico Tech Seismological

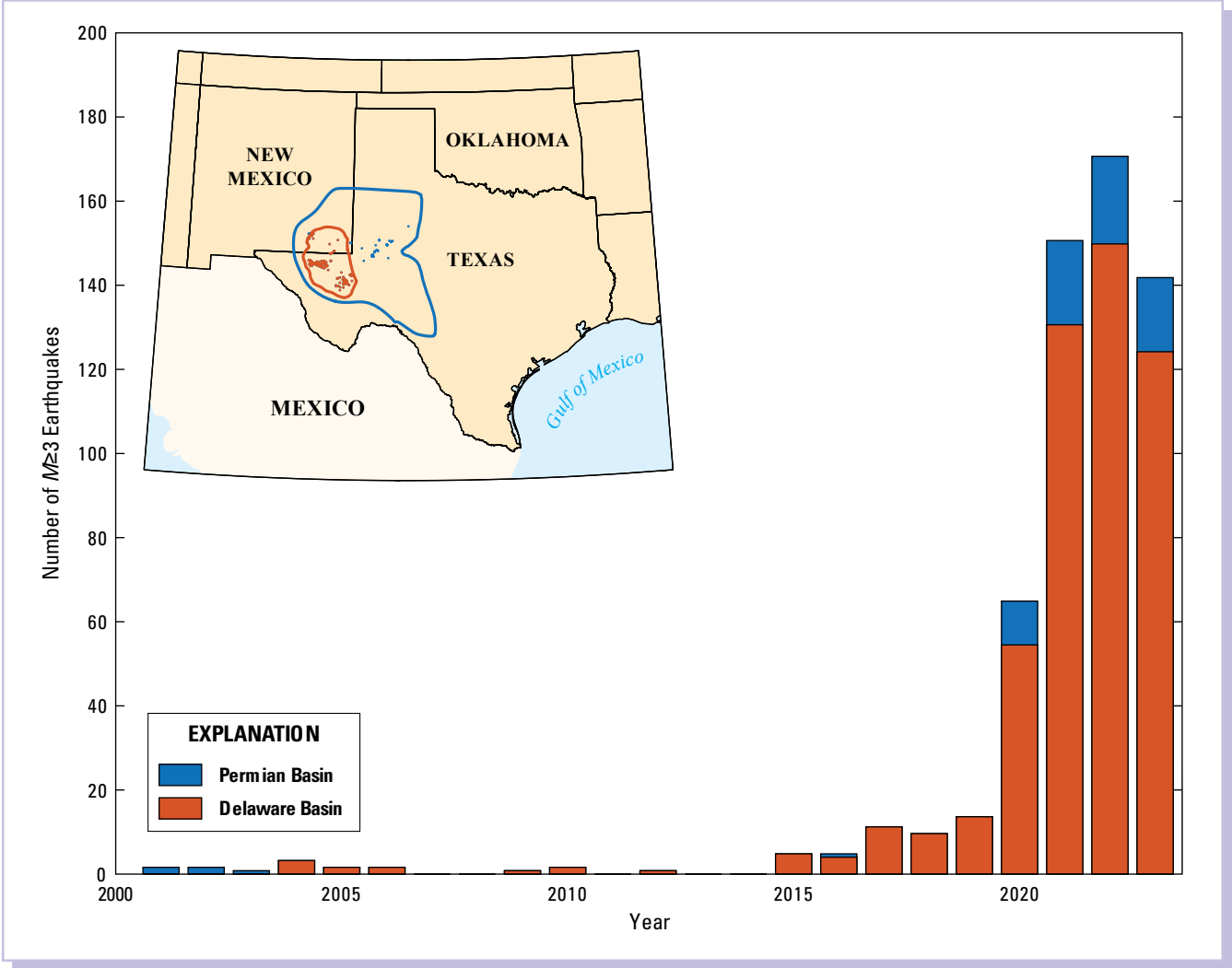


Figure 10. Bar graph showing seismicity rate increases in the region of the Permian Basin (blue), including the Delaware Basin (red), in parts of New Mexico and Texas since 2015 (U.S. Geological Survey, 2017). Inset map shows the locations of Permian (blue polygon) and Delaware (red polygon) Basins, with the locations of $M \geq 3$ earthquake epicenters within the Permian and Delaware Basins shown as blue and red points, respectively. Abbreviation: M , magnitude.

Observatory. The network has 14 stations in a 40 km by 50 km region, giving a station spacing of ~10 km. AQMS is used for near-real-time detection and location. In addition to routine earthquake detection and location, research could be conducted to explore the following subjects: the spatial and temporal evolution of the seismicity, source properties of the earthquakes, the relationship between seismicity and fluid injection, stress variability within the region, and clustering of seismicity. Monthly wastewater disposal volumes are made available by New Mexico's Energy, Minerals, and Natural Resources Department.

Without significant mitigation efforts made by either industry or regulators, seismicity in this region will likely continue at the same rate or increase beyond its current pace. Outside of the region covered by the New Mexico seismic deployment, the USGS has undertaken studies of the *M*5.0 Mentone earthquake and hydraulic fracturing induced seismicity in the Texas part of the Delaware Basin (Skoumal and others, 2020, 2021; Skoumal and Trugman, 2021). Given the likelihood of ongoing seismicity in this region, monitoring and research efforts in the area could continue to contribute to understanding the induced seismicity.

Frontier Observatory for Research in Geothermal Energy

The DOE-funded FORGE site in Utah is a laboratory where scientists and researchers learn how to engineer EGS and is the first dedicated field site of its kind. The goal of FORGE is to improve our fundamental understanding of the key mechanisms controlling EGS success; develop, test, and refine techniques in an ideal EGS environment; and rapidly disseminate technical data and communicate lessons learned and best practices to the public. EGS are different from conventional geothermal resources that occur naturally

in the United States and are geographically limited owing to the need for underground heat and fluids (Tester and others, 2007). EGS are manmade geothermal reservoirs and can be engineered in most parts of the country, potentially expanding geothermal energy production and transforming the domestic energy portfolio (Tester and others, 2007).

ISP is involved in two FORGE projects that run from 2022 to 2025. The first project considers an array of novel low-cost strain sensors to measure deformation of the field during stimulation and production. The second project considers laboratory experiments to investigate processes that heal faults and modify hydraulic diffusivity under hydrothermal conditions. Results from laboratory experiments can be incorporated in coupled thermal-hydraulic-mechanical-chemical models of geothermal reservoirs.

Limitations and Opportunities for Innovation

Limitations

Several factors exist that limit our ability to make progress on research on induced seismicity. The major limiting factor is data availability. The critical datasets, in order of priority, are composed of industrial, geological, and seismological data. In some instances, it may be important to look to analogous industry activities, such as the Paradox Basin injection site that injects natural brine from the Colorado River (King and others, 2016), to understand implications of long-term injection. Partnerships with international researchers and industry groups are also advantageous for instances in which more complete datasets are available.

Industrial Data

Industrial data— injection rates, pressures, depths, timing of hydraulic fracture stimulations—are all key sources of information for understanding and modeling induced seismicity. In most States, regulations are set by the State and, as such, these data are collected and distributed by different agencies with different rules and retrieval methods. In some States, for example, Oklahoma, wastewater disposal rates and pressures are reported and published daily to an accessible website (Oklahoma Corporation Commission, 2023). In California, the Department of Conservation maintains a similar, publicly accessible database that also includes data from geothermal fields (California Department of Conservation, 2023). In other States, data like these are not always as easily accessible. Building relationships with the State agencies responsible for both regulating the wells and maintaining the databases is critical for the USGS to conduct research and respond to instances of potentially induced seismicity on a rapid basis. The USGS has developed working relationships with regulators in several states and the EPA, which regulates on Tribal lands and in States that have chosen not to administer their own regulatory programs.

Maintaining relationships with industrial partners, including energy companies and food processing companies working towards net carbon neutrality, has been beneficial to placing of seismometers in regions of induced seismicity. Close working relationships with industry partners in GCS have yielded access to injection and pressure data, as well as access to deep borehole seismic data. Continued collaboration with industry has and can continue to provide access to high fidelity injection data. Highlighting areas of mutually beneficial research may be advantageous, such as determining the effects of different operational choices on expected induced seismicity rates.

Geological Data

High-resolution geological data of the subsurface are valuable to understanding induced seismicity. Energy companies often have additional geological data than what is available in the public domain. For example, scientists with the Oklahoma Geological Survey collaborated with industry to develop a fault map of Oklahoma that had a far higher density of faults than were previously in the public domain (Marsh and Holland, 2016). Several energy companies also shared stress measurements

with a research group from Stanford University, providing a far denser sampling of stress orientations in Oklahoma and Texas (Lund, Snee, and Zoback, 2016; Alt and Zoback, 2017). Industry also holds geological data at depth from drill cores that would also help to improve understanding of induced seismicity. The Illinois State Geological Survey shared various core samples from the Decatur, Ill. Site for testing of geomechanical and hydrologic parameters (Morrow and others, 2017). As shown by Morrow and others (2017), these samples improved the USGS’s understanding of the material properties in and near the injection formation and elucidated the geomechanical differences that lead to microseismicity in various formations. In some States, however, this type of information is not easily accessible; for instance, at geothermal fields in southern California, such information is generally considered proprietary, which makes it difficult to overcome certain simplifying assumptions in assessing what proportion of ground deformation is related to natural fault slip rather than reservoir depletion (for example, Barbour and others, 2016). Cooperation with industry partners has proven valuable to many induced seismicity studies in the past.

Seismological Data

The USGS’s ability to observe induced seismicity is limited by the density and quality of seismic networks in the areas of seismicity. Most of the recent induced seismicity has occurred in regions with few seismometers owing to low natural seismicity rates, such that our spatial resolution is poor, and we are unable to detect smaller events. New instances of induced seismicity are likely to continue to occur in locations where the seismological coverage is sparse. As such, catalogs for the early stages of induced seismicity will likely remain of relatively poor quality. To address this, various options are available to consider: densify seismic monitoring everywhere, which is likely unrealistic given funding constraints; target areas of expanding oil and gas operations with additional seismometers in the expectation of induced seismicity, although seismicity is not guaranteed to occur; or be prepared to respond quickly to areas where seismicity has begun occurring, although seismicity is not guaranteed to continue and the beginning of earthquake sequences will not be recorded.

Cooperation with state agencies with seismometers has been fruitful and allowed for the detection of more earthquakes than would otherwise be possible. Coordination with industry partners with installed private monitoring networks would be valuable in providing greater densities of stations.

Opportunities for Innovation

Oil and Gas

Ongoing and future opportunities for research in oil- and gas-related induced seismicity include improvements in developing and assessing induced seismicity forecasts, tracking the distribution and evolution of pore pressures in target reservoirs, examining the prevalence of aseismic slip and its impact on seismic slip occurrence, and field-scale experimenting of induced seismicity occurrence. Below are some fundamental questions and approaches related to understanding the physical processes and forecasting the expected hazard from oil- and gas-related induced seismicity:

- How can hazard forecasts be improved to provide more accurate estimates of rapidly changing induced seismicity hazards? Are physics-based forecasts that consider injection rate information to estimate stressing rate changes in addition to recent seismicity required to improve the prediction of seismicity rate increases and, just as critically, decreases? Do short-term earthquake rate forecasts produce more accurate forecasts than existing forecasts on 1-year timescales (Petersen and others, 2015)?
- What are the distributions of subsurface pore pressures and how do they evolve in regions of fluid disposal? Using data available from a single pore pressure sensor in Oklahoma, we were able to confirm long-term pressurization of the Arbuckle Group reservoir, the target of injection (Barbour and others, 2019). Barbour and others (2019) overturned the long-standing belief that the Arbuckle Group reservoir is confined, finding instead that it likely allows fluid to migrate into the basement. An azimuthally dependent poroelastic response was also documented with teleseismic surface waves (Barbour and Beeler, 2021). Additional subsurface pore pressure monitoring, especially near new and ongoing injection or hydraulic fracturing, would allow us to better constrain subsurface information critical to understanding and forecasting earthquake occurrence.
- What are the types of slip processes that can occur on faults affected by injection? USGS work on oil- and gas-related induced seismicity has primarily focused on seismic slip (earthquakes) caused by fluid injection, but recent studies indicate that fluid injection may also cause aseismic slip (for example, Guglielmi and others, 2015; Eyre and others, 2019). Geodetic data are typically used to identify aseismic slip, but the total amount of slip caused by local fluid injection is expected to be small and may not be visible on most geodetic measurements (GNSS, InSAR, and so on). Borehole strain measurements near active faults may provide useful insights but generally are not available. Recent technological advancements in fiber-optic strain sensing may help close this observational gap. Alternately, proxies for aseismic slip, such as repeating earthquakes that have been detected in areas of active injection, may be useful for establishing whether aseismic slip is common in regions with large-scale fluid injection.
- What approaches can improve the available data for understanding how and when induced seismicity occurs? In the 1960s and 1970s, the USGS led a study of induced seismicity by running an induced earthquake experiment to better understand the controls on earthquake occurrence (Raleigh and others, 1976). In recent years, induced seismicity researchers have proposed a new experiment to understand the controls on earthquake triggering by fluid injection (Savage and others, 2017). New instrumentation types (digital surface and borehole seismometers, nodal seismic sensors, borehole strainmeters, fiber-optic strain-sensing, and others) and approaches (template matching and machine learning-based event detection methods, imaging of small seismic source properties, inferring stress from focal mechanisms and shear wave splitting, and others) would provide a wealth of new data from cutting edge technologies not possible in those early experiments. Should such an experiment go forward, the USGS has a natural role to play in experiment design, data collection, and analysis.

Geothermal

Advancements in USGS research related to induced seismicity and ground deformation owing to geothermal energy operations could include spatial analysis of surface deformation, time evolution of surface deformation, new advancements in ground strain observing techniques, and site-specific and regional scale induced seismicity hazard analysis. Below we highlight opportunities for research into geothermal induced seismicity and ground deformation:

- Does the source of surface deformation at geothermal fields occur over reservoir scales, or is the source confined and localized on the basis of fault and (or) fracture and temperature structures? Recent observations of subsidence anomalies and induced seismicity rates indicate a complex association with injection and production volumes at geothermal fields in California. Analyses of surface deformation and seismicity patterns could benefit from advanced fault identification methods (for example, FaultID, Skoumal and others, 2019) to assess plausible sources of subsidence and seismic hazard, especially as a complement to advanced seismic detection methods (for example, template matching, Cochran and others, 2018, Skoumal and others, 2019).
- How can we better track the time evolution of ground deformation for validation of surface deformation modeling? Observationally, the development of time series of ground deformation over geothermal areas of interest would benefit the capture of long-term, steady deformation rates, as well as transient deformation (for example, in the case of Heber [Barbour, 2021]). These time series could be compared against the injection and production parameters of geothermal operations and THMC modeling results. With current InSAR and GNSS technologies, we have adequate observational capacity in arid environments, such as Coso, Calif. However, various challenges persist in agricultural regions like the Imperial Valley, Calif. And densely forested regions like The Geysers, Calif. With the launch of the NISAR mission in 2024 more comprehensive coverage may be acquired in such challenging regions (National Aeronautics and Space Administration, 2024).
- What approaches are needed to observe surface and subsurface strain rates? InSAR and GNSS time series could help to better understand long term and anomalous strain rates in the crust during geothermal activities, which could potentially point to mechanisms of stress transfer and seismicity generation. Geodesy is also one of the only ways to detect surface signals associated with deep aseismic slip; new fiber optic strain-sensing instruments under development could allow for measurements close to the source, including borehole optical fiber strainmeters (for example, De Wolf and others, 2019) and distributed acoustic sensing (for example, Lindsey and others, 2020). As these technologies develop further and become better tested in hydrothermal conditions, they may represent significant advancements in low-frequency signal detection at unprecedented resolution.
- How can site-specific and regional-scale hazard forecasts be improved? Geothermal resource development is expected to expand, and we foresee a demand for site-specific, pre-production induced seismicity hazard analysis and regional scale earthquake hazard forecasts near ongoing operations. Producing a map of earthquake hazards for geothermal resource development will require a multidisciplinary approach that considers important aspects such as cutting-edge research on background seismicity rates, ground motions and site response, maximum magnitudes (especially for induced earthquakes), strain rates, locations of preexisting faults and their scale and (or) slip rates, the proportion of the total moment released aseismically, fracture networks and their permeability structure, in-situ state of stress, physical and geomechanical rock properties, and hydrothermal conditions. Each of these topics is a focus of vigorous scientific research and is rife with both aleatoric and epistemic uncertainty. Thus, a comprehensive approach may support increased understanding of hazards and development of public-facing products related to geothermal deformation and seismicity hazards that address the needs of both stakeholders and the public.

Geologic CO₂ Sequestration

Ongoing and future opportunities for research in induced seismicity related to GCS include improvements in the understanding of the physical emplacement of CO₂ in the subsurface and how that differs from wastewater injection, establishing whether seismic methods can be utilized to improve CO₂ plume monitoring, and whether injection strategies can mitigate the seismic hazard posed by GCS. Specifically, the following are some fundamental questions addressing GCS-related induced seismicity:

- Can induced seismicity be mitigated by isolating the basement from significant pore pressure increases through injection into shallower, hydrologically separated reservoir horizons? Our findings (Kaven and others, 2014b; 2015b) in part motivated the shallower injection in the second phase during the ICCS project at Decatur, Ill. So far this mitigation strategy appears to have the intended consequences, in that microseismicity is lower in magnitude and frequency. However, additional site studies to further test this mitigation strategy may improve understanding of the mechanisms.
- How can knowledge of in-situ stress field, geohydrologic structure, rock mechanical properties, and injection parameters be used to understand the physical processes controlling induced seismicity associated with carbon capture and storage? Can this knowledge be used to change the operational parameters of CO₂ injection (for example, well configuration and wellhead injection rates and pressures) to reduce the seismic hazards posed by GCS?
- Can the location and extent of a CO₂ plume be reliably imaged? Operators of GCS sites are required to monitor the extent of this CO₂ plume for years after operations ends. For example, delineating the extent of the CO₂ plume at the Decatur, Ill., site using active seismic methods has proved difficult, as these methods have not yielded sufficient resolution. A novel approach to overcoming the lack of resolution of active seismic methods may be the use of ambient noise tomography (Ajo-Franklin and others, 2013). Ambient noise tomography is an emerging field in seismology that interrogates the temporal changes in the subsurface structure beneath pairs of seismometers by cross correlating the ambient noise field. The methods may shed light on density changes near GCS sites, which are expected as lower density, supercritical CO₂ is injected into higher density brine. If the potential of these methods can be realized in GCS settings, then these methods may significantly aid in monitoring and assessing the hazard associated with the plume dispersion.
- What modifications to hazard forecasting approaches are needed for application to GCS-related induced seismicity? The USGS has developed physics-based seismicity rate models for wastewater disposal operations and has shown the ability to forecast seismicity rates for operations in the central and eastern United States (Norbeck and Rubinstein, 2018). For a wide-spread, basin-wide adoption of GCS in, for example, the Illinois Basin, these methods hold great potential in achieving similar forecasting abilities. However, the two-phase nature of CO₂ injection and buoyancy of supercritical CO₂ poses additional complications to the physics involved in these methods. Using the Decatur, Ill., GCS site for calibration, these methods could potentially be extended to application in GCS settings and could similarly provide physics-based forecasts of seismicity rates and seismic hazard.

Summary

The strategic vision herein outlines strategic priorities and goals for induced seismicity research in the Earthquake Hazards Program of the U.S. Geological Survey during the next 5 years and beyond. In the past 15 years, the USGS expanded research activities related to induced earthquakes primarily through the Induced Seismicity Project within the Earthquake Science Center. These efforts include a robust field-monitoring program that collects seismic, geodetic, and pore-pressure data, as well as laboratory experiments on slip behavior and rock properties. Since the inception of the Induced Seismicity Project, we have developed a suite of capabilities to detect and characterize earthquakes, explore sequence behavior, identify subsurface fault structures, model pore pressure diffusion and deformation, and forecast wastewater disposal induced hazard. During the next five years work may continue to develop and apply these techniques as well as expand research into new focus areas such as the Permian Basin and the Utah Frontier Observatory for Research in Geothermal Energy site. Some impediments to progress remain, including having access to geologic and industrial data of sufficient detail, as well as adequate seismic monitoring, particularly in emerging areas of induced seismicity. This document is primarily focused on work that can be completed at existing funding levels, but a few potential opportunities to expand work in the future if resources allow are described.

References Cited

- Ajo-Franklin, J.B., Peterson, J., Doetsch, J., and Daley, T.M., 2013, High-resolution characterization of a CO₂ plume using crosswell seismic tomography—Cranfield, MS, USA: *International Journal of Greenhouse Gas Control*, v. 18, p. 497–509, <https://doi.org/10.1016/j.ijggc.2012.12.018>.
- Alt, R.C., and Zoback, M.D., 2017, In situ stress and active faulting in Oklahoma—*Bulletin of the Seismological Society of America*, v. 107, no. 1, p. 216–228, <https://doi.org/10.1785/0120160156>.
- Amemoutou, A., Martínez-Garzón, P., Kwiatak, G., Rubinstein, J.L., Bohnhoff, M., 2021, Earthquake source mechanisms and stress field variations associated with wastewater-induced seismicity in southern Kansas, USA: *Journal of Geophysical Research—Solid Earth*, v. 126, no. 7, e2020JB021625, <https://doi.org/10.1029/2020JB021625>.
- Baltay, A.S., and Abercrombie, R.E., 2020, Stress drop and ground-motion source comparison of the July 2019 Ridgecrest earthquake sequence—A community validation study *in* 2020 Southern California Earthquake Center Annual Meeting, virtual meeting: Southern California Earthquake Center, contribution #10673, poster #073.
- Barbour, A.J., 2021, Induced seismicity and deformation at Geothermal Fields in California, USA *in* *Proceedings World Geothermal Congress, Reykjavik, Iceland, October 24–27, 2021: World Geothermal Congress*, 11 p., accessed February 1, 2023, at https://www.geothermal-energy.org/cpdb/record_detail.php?id=32928.
- Barbour, A.J., and Beeler, N.M., 2021, Teleseismic waves reveal anisotropic poroelastic response of wastewater disposal reservoir: *Earth and Planetary Physics*, v. 5, no. 6, p. 547–558, <http://doi.org/10.26464/epp2021034>
- Barbour, A.J., Evans, E.L., Hickman, S.H., and Eneva, M., 2016, Subsidence rates at the southern Salton Sea consistent with reservoir depletion: *Journal of Geophysical Research—Solid Earth*, v. 121, no. 7, p. 5308–5327, <https://doi.org/10.1002/2016JB012903>.
- Barbour, A.J., Norbeck, J.H., and Rubinstein, J.L., 2017, The effects of varying injection rates in Osage County, Oklahoma, on the 2016 M5.8 Pawnee earthquake: *Seismological Research Letters*, v. 88, no. 4, p. 1040–1053, <https://doi.org/10.1785/0220170003>.
- Barbour, A.J., Xue, L., Roeloffs, E., and Rubinstein, J.L., 2019, Leakage and increasing fluid pressure detected in Oklahoma’s wastewater disposal reservoir—*Journal of Geophysical Research: Solid Earth*, v. 124, no. 3, p. 2896–2919, <https://doi.org/10.1029/2019JB017327>.
- Barnhart, W.D., Benz, H.M., Hayes, G.P., Rubinstein, J.L., and Bergman, E., 2014, Seismological and geodetic constraints on the 2011 Mw5.3 Trinidad, Colorado earthquake and induced deformation in the Raton Basin—*Journal of Geophysical Research: Solid Earth*, v. 119, no. 10, p. 7923–7933, <https://doi.org/10.1002/2014JB011227>.
- Barnhart, W.D., Yeck, W.L. and McNamara, D.E., 2018, Induced earthquake and liquefaction hazards in Oklahoma, USA: Constraints from InSAR—*Remote Sensing of Environment*, v. 218, p.1–12, <https://doi.org/10.1016/j.rse.2018.09.005>.
- Benson, S.M. and Cole, D.R., 2008, CO₂ sequestration in deep sedimentary formations: *Elements*, v. 4, no. 5, p. 325–331, <https://doi.org/10.2113/gselements.4.5.325>.

- Boak, J., 2016, Patterns of Induced Seismicity in central and northwest Oklahoma [abs], in SEG Technical Program Expanded Abstracts 2016, 87th Annual Society of Exploration Geophysics Meeting, Dallas, Tex., October 16–21, 2016, Abstracts: Society of Exploration Geophysics, p. 5039–5042, <https://doi.org/10.1190/segam2016-13960154.1>.
- Boyd, O.S., McNamara, D.E., Hartzell, S. and Choy, G., 2017, Influence of lithostatic stress on earthquake stress drops in North America: Bulletin of the Seismological Society of America, v. 107, no. 2, p. 856–868, <https://doi.org/10.1785/0120160219>.
- Brown, D., DuTeaux, R., Kruger, P., Swenson, D. and Yamaguchi, 1999, Fluid circulation and heat extraction from engineered geothermal reservoirs: Geothermics, v. 28, p. 553–572, [https://doi.org/10.1016/S0375-6505\(99\)00028-0](https://doi.org/10.1016/S0375-6505(99)00028-0).
- California Department of Conservation, 2023, Geologic Energy Management Division, accessed January 27, 2023, at <https://www.conservation.ca.gov/calgem>.
- Cochran, E.S., Ross, Z.E., Harrington, R.M., Dougherty, S.L. and Rubinstein, J.L., 2018, Induced earthquake families reveal distinctive evolutionary patterns near disposal wells: Journal of Geophysical Research—Solid Earth, v. 123, no. 9, p. 8045–8055, <https://doi.org/10.1029/2018JB016270>.
- Cochran, E.S., Skoumal, R.J., McPhillips, D., Ross, Z.E., and Keranen, K.M., 2020a, Activation of optimally and unfavourably oriented faults in a uniform local stress field during the 2011 Prague, Oklahoma, sequence: Geophysical Journal International, v. 222, no. 1, p. 153–168, <https://doi.org/10.1093/gji/ggaa153>.
- Cochran, E.S., Wickham-Piotrowski, A., Kemna, K.B., Harrington, R.M., Dougherty, S.L., and Peña Castro, A.F., 2020b, Minimal clustering of injection-induced earthquakes observed with a large-n seismic array: Bulletin of the Seismological Society of America, v. 110, no. 5, p. 2005–2017, <https://doi.org/10.1785/0120200101>.
- Delatte, N. and Greer, A., 2018, Earthquakes in Oklahoma—Adapting to a new reality: Forensic Engineering 2018: Forging Forensic Frontiers, p. 940–946, <https://doi.org/10.1061/9780784482018.090>.
- Dempsey, D., and Riffault, J., 2019, Response of induced seismicity to injection rate reduction—Models of delay, decay, quiescence, recovery, and Oklahoma: Water Resources Research, v. 55, no. 1, p. 656–681, <https://doi.org/10.1029/2018WR023587>.
- DeWolf, S., Murdoch, L., Germanovich, L., Moak, R., and Furgeson, M., 2019, Designs and results from three new borehole optical fiber tensor strainmeters [abs.], in American Geophysical Union Fall Meeting, San Francisco, CA, December 9–13, 2019, Abstract S21G-0597, <https://doi.org/10.1002/essoar.10501332.1>.
- Dougherty, S.L., Cochran, E.S. and Harrington, R.M., 2019, The LARge-n Seismic Survey in Oklahoma (LASSO): Seismological Research Letters, v. 90, no. 5, p. 2051–2057, <https://doi.org/10.1785/0220190094>.
- Ehrman, M.U., 2017, Earthquakes in the oilpatch: the regulatory and legal issues arising out of oil and gas operation induced seismicity [abs.], Georgia State University Law Review, v. 33, no. 3, p. 609–658, accessed January 30, 2023, at <https://ssrn.com/abstract=2761319>.
- Ellsworth, W., 2013, Injection-induced earthquakes: Science, v. 341, no. 6142, 7 p., <http://doi.org/10.1126/science.1225942>.
- Ellsworth, W.L., Giardini, D., Townend, J., Ge, S., and Shimamoto, T., 2019, Triggering of the Pohang, Korea, earthquake (Mw 5.5) by enhanced geothermal system stimulation: Seismological Research Letters, v. 90, no. 5, p. 1844–1858, <https://doi.org/10.1785/0220190102>.
- Eneva, M., Barbour, A.J., Adams, D., Hsiao, V., Blake, K., Falorni, F., and Locatelli, R., 2018, Satellite observations of surface deformation at the Coso Geothermal Field, California: Geothermal Resources Council Transactions, v. 42, p. 1383–1401, accessed 1/20/2023, at <https://publications.mygeoenergynow.org/grc/1033950.pdf>
- Eyre, T.S., Eaton, D.W., Garagash, D.I., Zecevic, M., Venieri, M., Weir, R., and Lawton, D.C., 2019, The role of aseismic slip in hydraulic fracturing-induced seismicity: Science, v. 5, no. 8, 10 p., <https://doi.org/10.1126/sciadv.aav7172>.
- Fasola, S.L., Brudzinski, M.R., Skoumal, R.J., Langenkamp, T., Currie, B.S., and Smart, K.J., 2019, Hydraulic fracture injection strategy influences the probability of earthquakes in the Eagle Ford Shale Play of South Texas: Geophysical Research Letters, v. 46, p. 12,958–12,967, <https://doi.org/10.1029/2019GL085167>.
- Folger, P. and Tiemann, M., 2016, Human-induced earthquakes from deep-well injection: A brief overview, Congressional Research Service, R43836, 29 p., accessed 1/12/2024, at <https://crsreports.congress.gov/product/pdf/R/R43836>.

- Galis, M., Ampuero, J.P., Mai, P.M., and Cappa, F., 2017, Induced seismicity provides insight into why earthquake ruptures stop: *Science Advances*, v. 3, no. 12, <https://doi.org/10.1126/sciadv.aap7528>.
- Ge, S. and Saar, 2022, M.O., Review: Induced seismicity during geoenery development—A hydromechanical perspective: *Journal of Geophysical Research—Solid Earth*, 127, e2021JB023141, <http://doi.org/10.1029/2021JB023141>.
- Greenberg, S., Whittaker, S. and McDonald, S., 2019, On the path to commercial CCS: Scaling from field demonstration to regional hub: Proceedings of the 14th Greenhouse Gas Control Technologies Conference, Melbourne, Australia 21-26 October 2018, <https://doi.org/10.2139/ssrn.3365965>.
- Grigoratos, I., Rathje, E., Bazzurro, P. and Savvaidis, A., 2020, Earthquakes induced by wastewater injection, Part I—Model development and hindcasting: *Bulletin of the Seismological Society of America*, v. 110, no. 5, p. 2466–2482, <https://doi.org/10.1785/0120200078>.
- Guglielmi, Y., Cappa, F., Avouac, J.-P., Henry, P., and Elsworth, D., 2015, Seismicity triggered by fluid injection-induced aseismic slip: *Science*, v. 348, no. 6240, p. 1224–1226, <https://doi.org/10.1126/science.aab0476>.
- Habermann, R.E., 1983, Teleseismic detection in the Aleutian Island Arc: *Journal of Geophysical Research—Solid Earth*, v. 88, no. B6, p. 5056–5064, <https://doi.org/10.1029/JB088iB06p05056>.
- Hartog, J.R., Friberg, P.A., Kress, V.C., Bodin, P., and Bhadha, R., 2020, Open-Source ANSS Quake Monitoring System Software: *Seismological Research Letters*, v. 91, no. 2A, p.677–686, <https://doi.org/10.1785/0220190219>.
- Healy, J.H., Rubey, W.W., Griggs, D.T. and Raleigh, C.B., 1968, The Denver Earthquakes: *Science*, v. 161, no. 3848, p.1301–1310, <https://doi.org/10.1126/science.161.3848.1301>.
- Hickman, S.H., 1991, Stress in the lithosphere and the strength of faults: *Reviews of Geophysics*, v. 29, p. 759–775.
- Hincks, T., Aspinall, W., Cooke, R. and Gernon, T., 2018, Oklahoma’s induced seismicity strongly linked to wastewater injection depth: *Science*, v. 359, no. 6381, p. 1251–1255, <https://doi.org/10.1126/science.aap7911>.
- Hough, S.E., 2014, Shaking from injection-induced earthquakes in the central and eastern United States. *Bulletin of the Seismological Society of America*, v. 104, no. 5, p. 2619–2626, <https://doi.org/10.1785/0120140099>.
- Jiang, G., Liu, L., Barbour, A.J., Lu, R., and Yang, H., 2021, Physics-based evaluation of the maximum magnitude of potential earthquakes induced by the Hutubi (China) underground gas storage: *Journal of Geophysical Research—Solid Earth*, v. 126, no. 4, e2020JB021379, <https://doi.org/10.1029/2020JB021379>.
- Joubert, C., Sohrabi, R., Rubinstein, J.L., Jansen, G. and Miller, S.A., 2020, Injection-induced earthquakes near Milan, Kansas, controlled by karstic networks. *Geophysical Research Letters*, v. 47, no. 21, e2020GL088326, <https://doi.org/10.1029/2020GL088326>.
- Kaven, J.O., 2020, Seismicity rate change at the Coso Geothermal Field following the July 2019 Ridgecrest earthquakes: *Bulletin of the Seismological Society of America*, v. 110, no.4, <https://doi.org/10.1785/0120200017>.
- Kaven, J.O., Hickman, S.H., and Davatzes, N.C., 2014a, Micro-seismicity and seismic moment release within the Coso Geothermal Field, California—Proceedings, 39th Workshop on Geothermal Reservoir Engineering: Stanford University, Stanford, California, 10 p., accessed 1/30/2023, at <https://pangea.stanford.edu/ERE/pdf/IGAstandard/SGW/2014/Kaven.pdf>.
- Kaven, J.O., Hickman, S.H., and Davatzes, N.C., 2015a, Seismicity and deformation in the Coso Geothermal Field from 2000 to 2012 [abs.], in *European Geosciences Union*, 12th, Vienna, Austria, April 12–17, 2015: EGU General Assembly Conference Abstracts, abs. no. 14466.
- Kaven, J.O., Hickman, S.H., McGarr, A.F. and Ellsworth, W.L., 2015b, Surface monitoring of microseismicity at the Decatur, Illinois, CO₂ sequestration demonstration site: *Seismological Research Letters*, v. 86, no. 4, p. 1096–1101, <https://doi.org/10.1785/0220150062>.
- Kaven, J.O., Hickman, S.H., McGarr, A.F., Walter, S. and Ellsworth, W.L., 2014b, Seismic monitoring at the Decatur, IL, CO₂ sequestration demonstration site, *Energy Procedia*, v. 63, p. 4264–4272, <https://doi.org/10.1016/j.egypro.2014.11.461>.
- Keranen, K.M., Weingarten, M., Abers, G.A., Bekins, B.A. and Ge, S., 2014, Sharp increase in central Oklahoma seismicity since 2008 induced by massive wastewater injection: *Science*, v. 345, no. 6195, p. 448–451, <https://doi.org/10.1126/science.1255802>.
- Kemna, K.B., Peña-Castro, A.F., Harrington, R.M. and Cochran, E.S., 2021, Using a large-n seismic array to explore the robustness of spectral estimations: *Geophysical Research Letters*, v. 47, no. 21, e2020GL089342, <https://doi.org/10.1029/2020GL089342>.

- King, V. M., L. V. Block, and C. K. Wood, 2016, Pressure/flow modeling and induced seismicity resulting from two decades of high-pressure deep-well brine injection, Paradox Valley, Colorado: *Geophysics*, v. 81, no. 5, p. B119–B134, <https://doi.org/10.1190/geo2015-0414.1>.
- Klara, S.M., Srivastava, R. D. and McIlvried, H. G., 2003, Integrated collaborative technology development program for CO2 sequestration in geologic formations – United States Department of Energy R&D: *Energy Conversion and Management*, v. 44, no. 17, p. 2699–2712, [https://doi.org/10.1016/S0196-8904\(03\)00042-6](https://doi.org/10.1016/S0196-8904(03)00042-6).
- Kim, K.-H., Ree, J.-H., Kim, Y., Kim, S., Kang, S.Y., Seo, W., 2018, Assessing whether the 2017 Mw5.4 Pohang earthquake in South Korea was an induced event: *Science*, v. 360, no. 6392, p. 1007–1009, <https://doi.org/10.1126/science.aat6081>.
- Konschnik, K., 2017, Regulating stability—state compensation funds for induced seismicity: *Georgetown Environmental Law Review*, v. 29, p. 227–300.
- Kroll, K.A., and Cochran, E.S., 2021, Stress controls rupture extent and maximum magnitude of induced earthquakes: *Geophysical Research Letters*, v. 48, no. 11, e2020GL092148, <https://doi.org/10.1029/2020GL092148>.
- Kwiatek, G., Saarno, T., Ader, T., Bluemle, F., Bohnhoff, M., Chendorain, M., Dresen, G., Heikkinen, P., Kukkonen, I., Leary, P., Leonhardt, M., Malin, P., Martínez-Garzón, P., Passmore, K., Passmore, P., Valenzuela, S., and Wollin, C., 2019, Controlling fluid-induced seismicity during a 6.1-km-deep geothermal simulation in Finland: *Science Advances*, v. 5, no. 5, <https://doi.org/10.1126/sciadv.aav7224>.
- Langenbruch, C., Weingarten, M. and Zoback, M.D., 2018, Physics-based forecasting of man-made earthquake hazards in Oklahoma and Kansas: *Nature Communications*, v. 9, no. 3946, p. 1–10, <https://doi.org/10.1038/s41467-018-06167-4>.
- Li, L., Tan, J., Schwarz, B., Stanek, F., Poiata, N., Shi, P., Diekmann, L., Eisner, L and Gajewski, D., 2020, Recent advances and challenges of waveform-based seismic location methods at multiple scales: *Reviews of Geophysics*, v. 58, no. e2019RG000667, <https://doi.org/10.1029/2019RG000667>.
- Lindsey, N.J., Rademacher, H., and Ajo-Franklin, J.B., 2020, On the broadband instrument response of fiber-optic DAS arrays: *Journal of Geophysical Research—Solid Earth*, v. 125, no. 2, e2019JB018145, <https://doi.org/10.1029/2019JB018145>.
- Liu, T., Luco, N., and Liel, A.B., 2019, Increases in life-safety risks to building occupants from induced earthquakes in the central United States: *Earthquake Spectra*, v. 35, no. 2, <https://doi.org/10.1193/041618EQS095M>.
- Llenos, A.L., and Michael, A.J., 2013, Modeling earthquake rate changes in Oklahoma and Arkansas—Possible signatures of induced seismicity: *Bulletin of the Seismological Society of America*, v. 103, no. 5, p. 2850–2861, <https://doi.org/10.1785/0120130017>.
- Llenos, A.L., and Michael, A.J., 2016, Characterizing potentially induced earthquake rate changes in the Brawley Seismic Zone, southern California: *Bulletin of the Seismological Society of America*, v. 106, no. 5, p. 2045–2062, <https://doi.org/10.1785/0120150053>.
- Llenos, A.L., and Michael, A.J., 2020, Regionally Optimized Background Earthquake Rates from ETAS (ROBERE) for probabilistic seismic hazard assessment: *Bulletin of the Seismological Society of America*, v. 110, no. 3, p. 1172–1190, <https://doi.org/10.1785/0120190279>.
- Llenos, A. L., and van der Elst, N. 2019, Improving earthquake forecasts during swarms with a duration model: *Bulletin of the Seismological Society of America*, v. 109, no. 3, p. 1148–1155, <https://doi.org/10.1785/0120180332>.
- Ludwig, K.A., Ramsey, D.W., Wood, N.J., Pennaz, A.B., Godt, J.W., Plant, N.G., Luco, N., Koenig, T.A., Hudnut, K.W., Davis, D.K., and Bright, P.R., 2018, Science for a risky world—A U.S. Geological Survey plan for risk research and applications: *U.S. Geological Survey Circular 1444*, 57 p., <https://doi.org/10.3133/cir1444>.
- Lund Snee, J.-E., and Zoback, M.D., 2016, State of stress in Texas—Implications for induced seismicity: *Geophysical Research Letters*, v. 43, no. 19, p. 10208–10214, <https://doi.org/10.1002/2016GL070974>.
- Majer, E., Nelson, J., Robertson-Tait, A., Savy, J. and Wong, I., 2013, Protocol for addressing induced seismicity associated with Enhanced Geothermal Systems: U.S. Department of Energy, DOE/EE-0662, 52 p., accessed January 12, 2024, at http://www1.eere.energy.gov/geothermal/pdfs/geothermal_seismicity_protocol_012012.pdf.
- Marsh, S., and Holland, A., 2016, Comprehensive fault database and interpretive fault map of Oklahoma: *Oklahoma Geological Survey Open-File Report, OF2-2016*, 15 p.
- Materna, K., Barbour, A., Jiang, J., and Eneva, M., 2022, Detection of aseismic slip and poroelastic reservoir deformation at the North Brawley Geothermal Field from 2009 to 2019: *Journal of Geophysical Research—Solid Earth*, v. 127, no. 5, e2021JB023335, <https://doi.org/10.1029/2021JB023335>.
- McGarr, A., Simpson, D. and L. Seeber, 2002, Case histories of induced and triggered seismicity: *International Geophysics*, v. 81A, p. 647–664, [https://doi.org/10.1016/S0074-6142\(02\)80243-1](https://doi.org/10.1016/S0074-6142(02)80243-1).

- McGarr, A., 2014, Maximum magnitude earthquakes induced by fluid injection: *Journal of Geophysical Research—Solid Earth*, v. 119, no. 2, p. 1008–1019, <https://doi.org/10.1002/2013JB010597>.
- McGarr, A., and Barbour, A.J., 2017, Wastewater disposal and the earthquake sequences during 2016 near Fairview, Pawnee, and Cushing, Oklahoma: *Geophysical Research Letters*, v. 44, no. 18, p. 9330–9336, <https://doi.org/10.1002/2017GL075258>.
- McGarr, A., and Barbour, A.J., 2018, Injection-induced moment release can also be aseismic. *Geophysical Research Letters*, v. 45, no. 11, p. 5344–5351, <https://doi.org/10.1029/2018GL078422>.
- McMahon, N.D., Aster, R.C., Yeck, W.L., McNamara, D.E., and Benz, H.M., 2017, Spatiotemporal evolution of the 2011 Prague, Oklahoma, aftershock sequence revealed using subspace detection and relocation—Prague, OK, aftershock sequence: *Geophysical Research Letters*, v. 44, no. 14, p. 7149–7158, <https://doi.org/10.1002/2017GL072944>.
- McNamara, D.E., Petersen, M.D., Thompson, E.M., Powers, P.M., Shumway, A.M., Hoover, S.M., Moschetti, M.P., and others, 2018, Evaluation of ground-motion models for USGS seismic hazard forecasts—induced and tectonic earthquakes in the central and eastern United States: *Bulletin of the Seismological Society of America*, v. 109, no. 1, p. 322–335. <https://doi.org/10.1785/0120180106>.
- Michael, A.J., McBride, S.K., Hardebeck, J.L., Barall, M., Martinez, E., Page, M.T., van der Elst, N., Field, E.H., Milner, K.R., and Wein, A.M., 2019, Statistical seismology and communication of the USGS Operational Aftershock Forecasts for the 30 November 2018 Mw 7.1 Anchorage, Alaska, earthquake: *Seismological Research Letters*, v. 91, no. 1, p. 153–173, <https://doi.org/10.1785/0220190196>.
- Morrow, C.A., Kaven, J.O., Moore, D.E., and Lockner, D.A., 2017, Physical properties of sidewall cores from Decatur, Illinois: U.S. Geological Survey, Open File Report 2017-1094, <https://doi.org/10.3133/ofr20171094>.
- Moschetti, M.P., Thompson, E.M., Powers, P.M., Hoover, S.M. and McNamara, D.E., 2019, Ground motions from induced earthquakes in Oklahoma and Kansas: *Seismological Research Letters*, v. 90, no. 1, p. 160–170, <https://doi.org/10.1785/0220180200>.
- Mousavi, S.M., Ellsworth, W.L., Zhu, W., Chuang, L.Y. and Beroza, G.C., 2020, Earthquake transformer—an attentive deep-learning model for simultaneous earthquake detection and phase picking: *Nature Communications*, v. 11, no. 3952, 12 p., <https://doi.org/10.1038/s41467-020-17591-w>.
- Murray, K., 2013, State-scale perspective on water use and production associated with oil and gas operations, Oklahoma, U.S.: *Environmental Science and Technology*, v. 47, no. 9, p. 4918–4925, <https://doi.org/10.1021/es4000593>.
- National Aeronautics and Space Administration, 2024, Jet Propulsion Laboratory: NISAR-ISRO SAR Mission, accessed 01/16/2024, <https://nisar.jpl.nasa.gov/>.
- National Research Council, 2013, *Induced seismicity potential in energy technologies*: National Academies Press, 62 p., [Also available at [https://yosemite.epa.gov/oa/eab_web_docket.nsf/Attachments%20By%20ParentFilingId/E928E3CEE612862D85257CD9006625A4/\\$FILE/Tab%20J1%20NAS%20Induced%20Seismicity%201%20of%205.pdf](https://yosemite.epa.gov/oa/eab_web_docket.nsf/Attachments%20By%20ParentFilingId/E928E3CEE612862D85257CD9006625A4/$FILE/Tab%20J1%20NAS%20Induced%20Seismicity%201%20of%205.pdf)].
- Newell, P. and Ilgen, A.G., 2019, Chapter 1 – Overview of Geological Carbon Storage (GCS): *Science of Carbon Storage in Deep Saline Formations*, p. 1–13, <https://doi.org/10.1016/B978-0-12-812752-0.00001-0>.
- Norbeck, J.H., and Rubinstein, J.L., 2018, Hydromechanical earthquake nucleation model forecasts onset, peak, and falling rates of induced seismicity in Oklahoma and Kansas: *Geophysical Research Letters*, v. 45, no. 7, p. 2963–2975, <https://doi.org/10.1002/2017GL076562>.
- Oklahoma Corporation Commission, 2023, Salt water disposal records: Oklahoma Corporation Commission database, accessed January 27, 2023, at <https://oklahoma.gov/occ/divisions/oil-gas/induced-seismicity-and-uic-department/salt-water-disposal-records-by-county.html>.
- Pennington, C.N., Chang, H., Rubinstein, J.L., Abercrombie, R.E., Nakata, N., Uchide, T., Cochran, E.S., 2022, Quantifying the sensitivity of microearthquake slip inversions to station distribution using a dense nodal array: *Bulletin of the Seismological Society of America*, v. 112, no. 3, p. 1252–1270, <https://doi.org/10.1785/0120210279>.
- Petersen, M.D., Mueller, C.S., Moschetti, M.P., Hoover, S.M., Rubinstein, J.L., Llenos, A.L., Michael, A.J., Ellsworth, W.L., McGarr, A.F., Holland, A.A., and Anderson, J.G., 2015, Incorporating induced seismicity in the 2014 United States national seismic hazard model—results of 2014 workshop and sensitivity studies: U.S. Geological Survey Open-File Report 2015-1070, 69 p., <https://doi.org/10.3133/ofr20151070>.
- Petersen, M.D., Mueller, C.S., Moschetti, M.P., Hoover, S.M., Llenos, A.L., Ellsworth, W.L., Michael, A.J., Rubinstein, J.L., McGarr, A.F., and Rukstales, K.S., 2016, 2016 One-year seismic hazard forecast for the central and eastern United States from induced and natural earthquakes: U.S. Geological Survey Open-File Report 2016-1035, 52 p., <https://doi.org/10.3133/ofr20161035>.

- Petersen, M.D., Mueller, C.S., Moschetti, M.P., Hoover, S.M., Rukstales, K.S., McNamara, D.E., Williams, R.A., and others, 2018, 2018 one-year seismic hazard forecast for the central and eastern United States from induced and natural earthquakes: *Seismological Research Letters*, v. 89, no. 3, p. 1049–1061, <https://doi.org/10.1785/0220180005>.
- Petersen, M.D., Mueller, C.S., Moschetti, M.P., Hoover, S.M., Shumway, A.M., McNamara, D.E., Williams, R.A., Llenos, A.L., Ellsworth, W.L., Michael, A.J., Rubinstein, J.L., McGarr, A.F., Rukstales, K.S., 2017, 2017 one-year seismic-hazard forecast for the central and eastern United States from induced and natural earthquakes: *Seismological Research Letters*, v. 88, no. 3, p. 772–783, <https://doi.org/10.1785/0220170005>.
- Proctor, B., Lockner, D.A., Kilgore, B., Mitchell, T.M., and Beeler, N.M., 2020, Direct evidence for fluid pressure, dilatancy, and compaction affecting slip in isolated faults: *Geophysical Research Letters*, v. 47, no. 16, e2019GL086767, <https://doi.org/10.1029/2019GL086767>.
- Raleigh, C. B., J. H. Healy, and J. D. Bredehoeft, 1976, An experiment in earthquake control at Rangely, Colorado., *Science*, 191, no. 4233, 1230–7, <https://doi.org/10.1126/science.191.4233.1230>.
- Reis, R., Brudzinski, M., Skoumal, R.J. and Currie, B.S., 2020, Factors influencing the probability of hydraulic fracturing-induced seismicity in Oklahoma: *Bulletin of the Seismological Society of America*, v. 110, no. 5, p. 2272–2282, <https://doi.org/10.1785/0120200105>.
- Rezaeian, S., Petersen, M.D., and Moschetti, M.P., Powers, P., Harmsen, S.C., Frankel, A.D., 2014, Implementation of NGA-West2 ground motion models in the 2014 U.S. national seismic hazard maps: *Earthquake Spectra*, v. 30, no. 3, p. 1319–1333, <https://doi.org/10.1193/062913EQS177M>.
- Roach, T., 2018, Oklahoma earthquakes and the price of oil: *Energy Policy*, v. 121, p. 365–373, <https://doi.org/10.1016/j.enpol.2018.05.040>.
- Ross, Z.E., Trugman, D.T., Hauksson, E. and Shearer, P.M., 2019, Searching for hidden earthquakes in southern California: *Science*, v. 364, no. 6442, p. 767–771, <https://doi.org/10.1126/science.aaw6888>.
- Rubinstein, J.L., Ellsworth, W.L., McGarr, A., and Benz, H.M., 2014, The 2001-present induced earthquake sequence in the Raton Basin of northern New Mexico and southern Colorado: *Bulletin of the Seismological Society of America*, v. 104, no. 5, p. 2162–2181, <https://doi.org/10.1785/0120140009>.
- Rubinstein, J.L., Ellsworth, W.L. and Dougherty, S.L., 2018, The 2013–2016 Induced earthquakes in Harper and Sumner Counties, southern Kansas: *Bulletin of the Seismological Society of America*, v. 108, no. 2, p. 674–689, <https://doi.org/10.1785/0120170209>.
- Rubinstein, J.L., and Mahani, A.B., 2015, Myths and facts on wastewater injection, hydraulic fracturing, enhanced oil recovery, and induced seismicity: *Seismological Research Letters*, v. 86, no. 4, p. 1060–1067, <https://doi.org/10.1785/0220150067>.
- Rubinstein, J.L., Barbour, A.J., and Norbeck, J.H., 2021, Forecasting induced earthquake hazard using a hydromechanical earthquake nucleation model: *Seismological Research Letters*, v. 92, no. 4, p. 2206–2220, <https://doi.org/10.1785/0220200215>.
- Sanchez, D.L., Johnson, N., McCoy, S.T. and Mach, K.J., 2018, Near-term deployment of carbon capture and sequestration from biorefineries in the United States: *Proceedings of the National Academy of Sciences*, v. 115, no. 19, p. 4875–4880, <https://doi.org/10.1073/pnas.1719695115>.
- Savage, H.M., Kirkpatrick, J.D., Mori, J.J., Brodsky, E.E., Ellsworth, W.L., Carpenter, B.M., Chen, X., Cappa, F., and Kano, Y., 2017, Scientific exploration of induced seismicity and stress (SEISMS): *Scientific Drilling*, v. 23, p. 57–63, <https://doi.org/10.5194/sd-23-57-2017>.
- Schoenball, M., Davatzes, N.C. and Glen, J.M.G., 2015, Differentiating induced and natural seismicity using space-time statistics applied to the Coso Geothermal field: *Geophysical Research Letters*, v. 42, no. 15, p. 6221–6228, <https://doi.org/10.1002/2015GL064772>.
- Schoenball, M., and Ellsworth, W.L., 2017, A systematic assessment of the spatiotemporal evolution of fault activation through induced seismicity in Oklahoma and southern Kansas: *Journal of Geophysical Research—Solid Earth*, v. 122, no. 12, p. 10189–10206, <https://doi.org/10.1002/2017JB014850>.
- Seismological Facility for the Advancement of Geoscience (SAGE), 2024, accessed January 16, 2024, at <https://iris.edu/hq/sage>.
- Shapiro, S.A., and Dinske, C., 2009, Scaling of seismicity induced by nonlinear fluid-rock interaction: *Journal of Geophysical Research—Solid Earth*, v. 114, no. B9, <https://doi.org/10.1029/2008JB006145>.
- Sharmin, T., Khan, N.R., Akram, M.S., Ehsan, Shelly, D.R., Hardebeck, J.L., Ellsworth, W.L., and Hill, D.P., 2016, A new strategy for earthquake focal mechanisms using waveform-correlation-derived relative polarities and cluster analysis—Application to the 2014 Long Valley Caldera earthquake swarm: *Journal of Geophysical Research—Solid Earth*, v. 121, no. 12, p. 8622–8641, <https://doi.org/10.1002/2016JB013437>.

- Shirzaei, M., Ellsworth, W.L., Tiampo, K.F., González, P.J., and Manga, M., 2016, Surface uplift and time-dependent seismic hazard due to fluid injection in eastern Texas: *Science*, v. 353, no. 6306, p.1416–1419, <https://doi.org/10.1126/science.aag0262>.
- Skoumal, R.J., Ries, R., Brudzinski, M.R., Barbour, A.J., and Currie, B.S., 2018, Earthquakes induced by hydraulic fracturing are pervasive in Oklahoma: *Journal of Geophysical Research—Solid Earth*, v. 123, no. 12, p. 10918–10935, <https://doi.org/10.1029/2018JB016790>.
- Skoumal, R.J., Kaven, J.O., and Walter, J.I., 2019, Characterizing seismogenic fault structures in Oklahoma using a relocated template-matched catalog: *Seismological Research Letters*, v. 90, no. 4, p. 1535–1543, <https://doi.org/10.1785/0220190045>.
- Skoumal, R.J., Barbour, A.J., Brudzinski, M.R., Langenkamp, T., and Kaven, J.O., 2020, Induced seismicity in the Delaware Basin, Texas: *Journal of Geophysical Research—Solid Earth*, v. 125, no. 1, e2019JB018558, <https://doi.org/10.1029/2019JB018558>.
- Skoumal, R.J., Cochran, E.S., Kroll, K.A., Rubinstein, J.L., and McPhillips, D., 2021a, Characterizing stress orientations in southern Kansas: *Bulletin of the Seismological Society of America*, v. 111, no. 3, p. 1445–1454, <https://doi.org/10.1785/0120200340>.
- Skoumal, R.J., Kaven, J.O., Barbour, A.J., Wicks, C., Brudzinski, M.R., Cochran, E.S., and Rubinstein, J.L., 2021b, The induced Mw 5.0 March 2020 west Texas seismic sequence: *Journal of Geophysical Research—Solid Earth*, v. 126, no. 1, e2020JB020693, <https://doi.org/10.1029/2020JB020693>.
- Skoumal, R.J., and Trugman, D.T., 2021, The proliferation of induced seismicity in the Permian Basin, Texas: *Journal of Geophysical Research—Solid Earth*, v. 126, no. 6, 16 p., e2021JB021921, <https://doi.org/10.1029/2021JB021921>.
- Suckale, J., 2009, Induced seismicity in hydrocarbon fields: *Advances in Geophysics*, v. 51, p. 55–106, [https://doi.org/10.1016/S0065-2687\(09\)05107-3](https://doi.org/10.1016/S0065-2687(09)05107-3).
- Sumy, D.F., Cochran, E.S., Keranen, K.M., Wei, M., and Abers, G.A., 2014, Observations of static Coulomb stress triggering of the November 2011 M 5.7 Oklahoma earthquake sequence: *Journal of Geophysical Research—Solid Earth*, v. 119, no. 3, p. 1904–1923, <https://doi.org/10.1002/2013JB010612>.
- Sumy, D.F., Neighbors, C.J., Cochran, E.S., and Keranen, K.M., 2017, Low stress drops observed for aftershocks of the 2011 M_w 5.7 Prague, Oklahoma, earthquake: *Journal of Geophysical Research—Solid Earth*, v. 122, no. 5, p. 3813–3834, <https://doi.org/10.1002/2016JB013153>.
- Teng, G., and Baker, J.W., 2019, Seismicity declustering and hazard analysis of the Oklahoma-Kansas region: *Bulletin of the Seismological Society of America*, v. 109, no. 6, p. 2356–2366, <https://doi.org/10.1785/0120190111>.
- Tester, J.W., Anderson, B.J., Batchelor, A.S., Balckwell, d.D., DiPippo, R., Drake, E.M., Garnish, J., Livesay, B., Moore, M.C., Nichols, K., Petty, S., Toksoz, M.N., Weatch, R.W., Baria, R., Augustine, C., Murphy, E., Negraru, P. and Richards, M., 2007, Impact of enhanced geothermal systems on the US energy supply in the twenty-first century: *Philosophical Transactions of the Royal Society A – Mathematical, Physical and Engineering Sciences*, v. 365, 1057–1094, <http://doi.org/10.1098/rsta.2006.1964>.
- Trugman, D.T., Dougherty, S.L., Cochran, E.S. and Shearer, P.M., 2017, Source spectral properties of small to moderate earthquakes in southern Kansas: *Journal of Geophysical Research—Solid Earth*, v. 122, no. 10, p. 8021–8034, <https://doi.org/10.1002/2017JB014649>.
- University of Texas, 2024, Bureau of Economic Geology: Texas seismological network and seismology research (TexNet), accessed January 16, 2024, at <https://www.beg.utexas.edu/texnet-cisr/texnet>.
- U.S. Department of Energy, 2024, FORGE phases and sites, accessed January 16, 2024, at <https://www.energy.gov/eere/geothermal/forge-phases-and-sites>.
- U.S. Energy Information Administration, 2022a, California State Energy Profile: U.S. Energy Information Administration database, accessed January 25, 2022, at <https://www.eia.gov/state/print.php?sid=CA>.
- U.S. Energy Information Administration, 2022b, Nevada State Energy Profile: U.S. Energy Information Administration database, accessed January 25, 2022, at <https://www.eia.gov/state/print.php?sid=NV>.
- U.S. Energy Information Administration, 2022c, Texas State Energy Profile: U.S. Energy Information Administration database, accessed January 25, 2022, at <https://www.eia.gov/state/print.php?sid=TX>.
- U.S. Environmental Protection Agency, 2022, Class VI Wells Permitted by EPA: U.S. Environmental Protection Agency database, accessed April 1, 2022, at <https://www.epa.gov/uic/class-vi-wells-permitted-epa>.
- U.S. Geological Survey, 2016, USGS water data for the Nation: U.S. Geological Survey National Water Information System database, accessed January 25, 2022, at <https://waterdata.usgs.gov/nwis>.
- U.S. Geological Survey, 2017, Advanced National Seismic System (ANSS) Comprehensive Earthquake Catalog: U.S. Geological Survey database, accessed January 25, 2022, at <https://earthquake.usgs.gov/data/comcat/>.

- Van der Elst, N.J., Page, M.T., Weiser, D.A., Goebel, T.H.W., and Hosseini, S.M., 2016, Induced earthquake magnitudes are as large as (statistically) expected: *Journal of Geophysical Research—Solid Earth*, v. 121, no. 6, p. 4575–4590, <https://doi.org/10.1002/2016JB012818>.
- Viets, V.F., Vaughan, C.K. and R.C. Harding, 1979, Environmental and economic effects of subsidence: Geothermal subsidence research management program, Lawrence Berkeley Laboratory Report, LBL-8615, 250 p., accessed January 16, 2024, at <https://escholarship.org/uc/item/1sb4c8vh>.
- Wang, C.-Y., Doan, M.-L., Xue, L., and Barbour, A.J., 2018, Tidal response of groundwater in a leaky aquifer—Application to Oklahoma: *Water Resources Research*, v. 54, no. 10, p. 8019–8033, <https://doi.org/10.1029/2018WR022793>.
- Wang, S., Jiang, G., Lei, X., Barbour, A.J., Tan, X., Xu, C., and Xu, X., 2022, Three $M_w \geq 4.7$ earthquakes within the Changning (China) shale gas field ruptured shallow faults intersecting with hydraulic fracturing wells: *Journal of Geophysical Research—Solid Earth*, v. 127, no. 2, e2021JB022946, <https://doi.org/10.1029/2021JB022946>.
- Way, H.S.K., 1983, Structural study of the Hunton Lime of the Wilzetta Field T12-13N, R5E, Lincoln County, Oklahoma, pertaining to the exploration for hydrocarbons: Stillwater, Oklahoma, Oklahoma State University, master thesis, 39 p., accessed February 10, 2022, at <https://shareok.org/handle/11244/16448>.
- Weingarten, M., Ge, S., Godt, J.W., Bekins, B.A. and Rubinstein, J.L., 2015, High-rate injection is associated with the increase in U.S. mid-continent seismicity: *Science*, v. 348, no. 6241, p. 1336–1340, <https://doi.org/10.1126/science.aab1345>.
- Wetherell, D. and Evensen, D., 2016, The insurance industry and unconventional gas development—Gaps and recommendations: *Energy Policy*, v. 94, p. 331–335, <https://doi.org/10.1016/j.enpol.2016.04.028>.
- White, I.J.O., Liu, T., Luco, N., and Liel, A., 2017, Considerations in comparing the U.S. Geological Survey one-year induced-seismicity hazard models with “Did You Feel It?” and instrumental data: *Seismological Research Letters*, v. 89, no. 1, p. 127–137, <https://doi.org/10.1785/0220170033>.
- White, J. A. and Foxall, W., 2016, Assessing induced seismicity risk at CO₂ storage projects: Recent progress and remaining challenges: *International Journal of Greenhouse Gas Control*, v. 49, p. 413–424, <https://doi.org/10.1016/j.ijggc.2016.03.021>.
- Woo, J.-U., Kim, M., Sheen, D.-H., Kang, T.-S., Rhie, J., Grigoli, F., Ellsworth, W.L., and Giardini, D., 2019, An in-depth seismological analysis revealing a causal link between the 2017 M_w 5.5 Pohang earthquake and EGS project: *Journal of Geophysical Research—Solid Earth*, v. 124, no. 12, p. 13060–13078, <https://doi.org/10.1029/2019JB018368>.
- Yeck, W.L., Block, L.V., Wood, C.K. and King, V.M., 2015, Maximum magnitude estimations of induced earthquakes at Paradox Valley, Colorado, from cumulative injection volume and geometry of seismicity clusters: *Geophysical Journal International*, v. 200, no. 1, p. 322–336. <https://doi.org/10.1093/gji/ggu394>.
- Yeck, W.L., Weingarten, M., Benz, H.M., McNamara, D.E., Bergman, E.A., Herrmann, R.B., Rubinstein, J.L., and Earle, P.S., 2016, Far-field pressurization likely caused one of the largest injection induced earthquakes by reactivating a large preexisting basement fault structure: *Geophysical Research Letters*, v. 43, no. 19, p. 10198–10207, <https://doi.org/10.1002/2016GL070861>.
- Zang, A., Oye, V., Jousset, P., Deichmann, N., Gritto, R., McGarr, A., Majer, E. and Bruhn, D., 2014, Analysis of induced seismicity in geothermal reservoirs—An overview: *Geothermics*, v. 52, p. 6–21, <https://doi.org/10.1016/j.geothermics.2014.06.005>.
- Zhai, G., Shirzaei, M., Manga, M., and Chen, X., 2019, Pore-pressure diffusion, enhanced by poroelastic stresses, controls induced seismicity in Oklahoma: *Proceedings of the National Academy of Sciences*, v. 116, no. 33, p. 16228–16233, <https://doi.org/10.1073/pnas.1819225116>.
- Ziagos, J., Phillips, B.R., Boyd, L., Jelacic, A., Stillman, G. and Hass, R., 2013, An Overview of the EGS Collab Project: Field Validation of Coupled Process Modeling of Fracturing and Fluid Flow at the Sanford Underground Research Facility, Lead, SD: *Proceedings of the Thirty-Eighth Workshop on Geothermal Reservoir Engineering*, Stanford University, Stanford, California, SGT-TR-198.
- Zoback, M.D. and Gorelick, S.M., 2012, Earthquake triggering and large-scale geologic storage of carbon dioxide: *Proceedings of the National Academy of Sciences*, v. 109, no. 26, <https://doi.org/10.1073/pnas.1202473109>.
- Zöller, G., and Holschneider, M., 2016, The maximum possible and the maximum expected earthquake magnitude for production-induced earthquakes at the gas field in Groningen, The Netherlands: *Bulletin of the Seismological Society of America*, v. 106, no. 6, p. 2917–2921, <https://doi.org/10.1785/0120160220>.

Publishing support provided by the Moffett Field Publishing Service Center
Manuscript approved May 19, 2023
Edited by Alex Lyles
Illustration support by Katie Sullivan
Graphic design and layout by Kimber Petersen

